Decoding cortical activity evoked by artificial retinal implants

Teva Andréoletti, Bruno Cessac, Frédéric Chavane

1st-Year Master's Internship

prepared at

INSTITUT NATIONAL DE RECHERCHE EN INFORMATIQUE ET EN AUTOMATIQUE

and defended at

ÉCOLE NATIONALE SUPÉRIEURE DE L'ÉLECTRONIQUE ET DE SES APPLICATIONS

Decoding cortical activity evoked by artificial retinal implants

By

Teva ANDRÉOLETTI

Supervisors:

M. Bruno CESSAC — INRIA Sophia Antipolis

M. Frédéric CHAVANE — INT Marseille

Mme. E. Veronica BELMEGA — ENSEA Cergy

April-August 2018, 2^{e} année (2017-2018 - Promo 2019)

2004 Route des Lucioles,
06902 Valbonne

Faculté de Médecine,
27 Boulevard Jean Moulin,
13005 Marseille

6 Avenue du Ponceau,
95000 Cergy

PREAMBLE

This study was carried out as part of the second year of study at ENSEA, and more specifically during the end-of-year internship.

Its purpose is to better understand the activity evoked by stimulation of the retina with implanted retinal prostheses used to partially restore sight in blind patients suffering from retinal degeneration.

The internship has been done in collaboration between Bruno Cessac (Biovision, INRIA, Sophia-Antipolis) and Frédéric Chavane (INT, CNRS, Marseille).

Contents

Acknowledgements

I would like to thank the entire BIOVISION team as well as the people I met during my visits to the INT Marseille, who allowed me to discover a warm and friendly working environment. The account of their experiences in the field of Research or during their studies was for me a real source of thinking for my professional project, and thanks to their friendship my internship's benefits are beyond my first expectations.

I would like to particularly thank Bruno Cessac and Frédéric Chavane for allowing me to do this internship. The passion they have for their job and the enthusiasm they show when they talk about it was one of the main factors in my motivation.

Finally, a big thank you to Selma Souihel for her daily support as well as her help with the sticking points I encountered.

List of Figures

GENERAL INTRODUCTION

Context

In an aging society like France's, diseases like AMD (Age-related Macular Degeneration) are increasingly present and require treatment. Because visual impairment is such a major global health issue, research in this area is essential.

And with over 280 millions of people living with a visual impairment due to pathologies of the retina, scientific interest in understanding how those diseases impact on the visual system has increased in the last years. Although the majority of these impairments are preventable or curable (such as the cataract which is a clouding of the lens in the eye leading to a decrease in vision), retinal degeneration disorders had no cure until recently.

With this in mind, one of the objectives of the NeOpTo team at INT Marseille and the BIOVISION team at INRIA is to improve prosthetic vision through cortical imaging and computational science.

Indeed, the increase of our knowledge in this field is one of the factors which, at the same level as the development of new technologies, will bring progress in the adaptation of fundamental research to tools improving the sight of visually impaired people with a vision that can only improve.

The internship

The visual system consists of many elements, all of which interpret the coded information from visible light in order to reconstruct our environment. The light enters through the eye and is projected onto its fundus, called the retina. The retina converts this information into an electrical signal using a principle called phototransduction. This signal is then transmitted through the optic nerve to the thalamus, one of whose main functions is to relay sensory signals to the visual cortex. Descriptions of the major elements of visual recognition will be given in Part I.

However, several factors can affect the functioning of the visual system. Among

them, many pathologies of the retina. Some of these degenerations, such as *Macular Degeneration* and *Retinitis Pigmentosa*, may lead to blindness. Nevertheless, new techniques have begun to be used to partly compensate these disorders (chapter 3).

Retinal implants are electronic devices attached to the retina that substitute to defective cells in order to partially restore vision. The principle is as follows: images acquired by a "camera + processor" system are encoded and sent as pulses to matrix of electrodes. It then stimulates the still functional cells of the retina in order to reproduce a luminous impression. Unfortunately, these prostheses have several limitations that will be discuss later (see subsection 3.2.4).

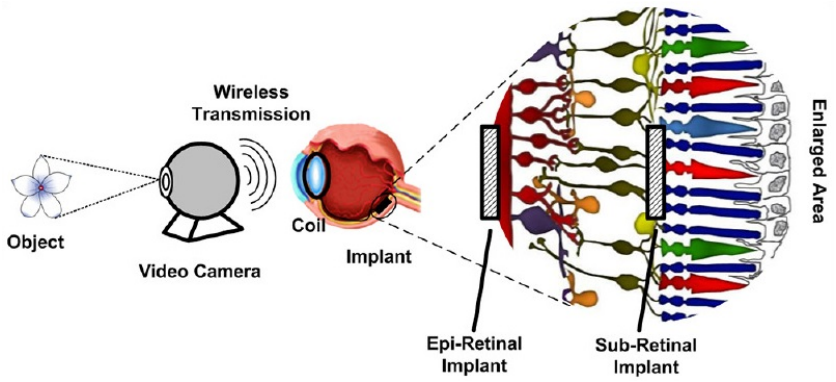

Figure 1 – Chain of function of retinal prostheses. Two types of retinal electrical implant (epiretinal or subretinal) are shown on the enlarged area (*Source: Journal of ophthalmic & vision research website*)

Among those limitations, it is difficult to target specific cells in the retina because of the larger electrode size. When an electrical pulse is sent to the visual cortex, what is called a *phosphene* is observed. This is a luminous activation point in the visual field that corresponds to the spatial location of the pulse. However, recent results in F. Chavane team on local stimulation of the retina showed evoked phosphene that are up to 10 times larger than what was expected, based on the activity evoked by visual stimuli, leading to a severe loss of visual resolution [1].

This observed spread of evoked cortical activity is presumably due to four effects: (i) an electric diffusion at the interface implant-retina; (ii) a spread of electric activity induced by the activation of retinal cells axons near the implant; (iii) an electric diffusion in the visual cortex and (iv) the optical diffusion of the signal registered by optical imaging.

In order to help understand the origin of the observed diffusion, a simulation model was developed by F. Chavane (see Part III). First, the retinal activation is modeled to take into account the diffusion effects (i) and (ii). In a second step, the diffusion effects (iii) and (iv) are applied to the activation profile obtained after

retino-cortical transformation. This model aims to quantify these four diffusive effects and more especially to analyse the role played by the retina's network (diffusive effect (ii)) in the spread of activity, by comparing the results of the model with the experimental results.

Thus, the subject of the internship was to reuse this model in order to find the results already obtained while modifying the program to optimize it; then finally to improve it in order to be able to compare the result obtained with experimental data.

Finally, this preliminary study was carried out on the rat but retinal prostheses are a priori implanted in humans. The interest is now to carried out the same experiments in animals closer to humans.

However,

Presentation of the INRIA and of the Institut des Neurosciences de la Timone (INT)

This internship, a collaboration between INRIA and INT, allowed me to learn more about these two institutions. If the majority of the internship took place on the INRIA site, my few visits to INT Marseille gave me the opportunity to really see the differences that can exist between two environment of work with the same purpose: Research.

INRIA

INRIA, Institut National de Recherche en Informatique et en Automatique, is a French institution dedicated to computational sciences which was created in 1967. There are 8 research centers in France, with more than 180 project-teams, in the following fields :

- Applied Mathematics, Computation and Simulation;
- Algorithmics, Programming, Software and Architecture;
- Networks, Systems and Services, Distributed Computing;
- Perception, Cognition and Interaction;
- Digital Health, Biology and Earth.

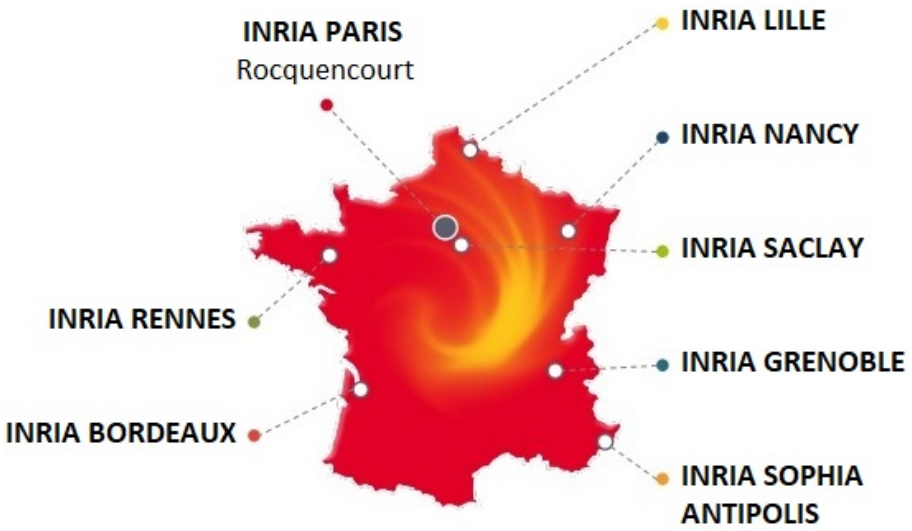

Figure 2 – Map of the INRIA research centers (*Source: conf-ng.jres.org / JRES 2015 "Le centre de services d'Inria et ses outils"*).

The Inria Sophia Antipolis - Méditerranée research center

Since 1983, the Inria Sophia Antipolis - Méditerranée research center, with its research teams based in Nice-Sophia Antipolis, Montpellier, Bologna (Italy) and Athens (Greece), is one of the major players in the European research area.

The center has not only research-oriented objectives but also entrepreneurial ones. It has 33 research teams, and 25 start-ups have been created in its incubator since 2005. This makes it possible to industrialize products from research prototypes, while disseminating the know-how acquired at the institute.

Nearly half of the research teams are mixed with one or more partners (the University of Côte d'Azur, CNRS, etc.). Nevertheless it does not stop there, since it also has many international partnerships. Moreover, organisms such as the ANR (The French National Research Agency) and the ERC (European Research Counsil) are really important since they help public research organisations, universities and even private companies by funding projects in all fields of science - for both basic and applied research.

The BIOVISION team

Among the 29 teams that are located in the Sophia-Antipolis center, my internship was affiliated to the BIOVISION team created in 2017.

Its theme is *Computational Neuroscience and Medicine* and the acronym means: *"**B**iologically plausible **I**ntegrative m**O**dels of the **V**isual system : towards synerg**I**stic **S**olutions for visually-**I**mpaired people and artificial visi**ON**"*.

People with vision loss due to retina impairments either have a certain degree of vision loss, low vision or even blindness.

The purpose of the BIOVISION team is to better understand biological vision through fundamental research as well as innovative technological developments in order to develop tools that will enable people with visual impairments to regain sufficient vision for their daily lives.

Website : https://team.inria.fr/biovision

INT

The INT, Institut de Neurosciences de la Timone, is a French institution dedicated to computational sciences which was created in 2011. It is a research unit of the University of Aix-Marseille and CNRS (National Center for Scientific Research). The CNRS is the largest governmental research organisation in France and the largest

fundamental science agency in Europe.

In order to bridge the gap between fundamental and clinical research, INT conducts world-class research in fundamental neuroscience, from the cellular to the cognitive level.

The main thematic axes to which the institute devotes itself deal with the understanding of: the dynamics of motor control (spinal and cortical systems), the perception systems (audition, vision) and the behavioral regulation systems (emotion, motivation).

Moreover, the institute hosts eleven research teams and has six technological platforms such as the molecular and cellular neurosciences platform or the in vivo and in vitro neuronal photon imaging platform.

The presence of these technological platforms in the same building makes it possible to handle a wide variety of interdisciplinary projects in the following fields:

- Neurophysiology;
- Cellular, Cognitive and Behavioural Neurosciences;
- Photonic Neuroimaging.

Website : http://www.int.univ-amu.fr/

The NeOpTo team

The NeOpTo team aims at elucidating the neural computations that underlies active vision. Even if vision is a major sensory input that guids our actions, helps us perceive our environment and conduct cognitive tasks, the visual inputs that reach the brain represent a computational challenge due to their complexity and dynamics. To investigate the functioning of the visual system, the NeOpTo team combines multiple expertises involving behavioral studies in both humans and monkeys, ophthalmologic clinical approaches and electrophysiological and real-time optical imaging studies in behaving monkeys.

Part I

Fundations

Chapter 1

The visual system

This chapter gives an overview of the structure of the visual system. In Section 1.1, the visual pathway is described. Sections 1.2 to 4.1 focus on the description of each part of the visual system.

1.1 The visual pathway

The visual system is the set of organs involved in the processing of visual information, from the eye to the visual cortex. A diagram of the visual pathway is given in the Figure 1.1. It is a detailed diagram that gives not only the main elements responsible for visual recognition, but also the evolution of the visual field projection from the retina to the visual cortex via the thalamus. This diagram has been very useful in understanding the visual system.

Light penetrates the eye and passes through it to the photosensitive cells of the retina on which the inverted image of the visual field is projected. The photons are then converted into electrical signals and transmitted to the brain by the optic nerve to the visual cortex, for interpretation.

1.2 The anatomy of the eye

Light enters the eye through the cornea, through the pupil and then through the lens. Accommodation corresponds to the lens shape change and is controlled by the ciliary muscle. It allows to change the focus position of the lens.

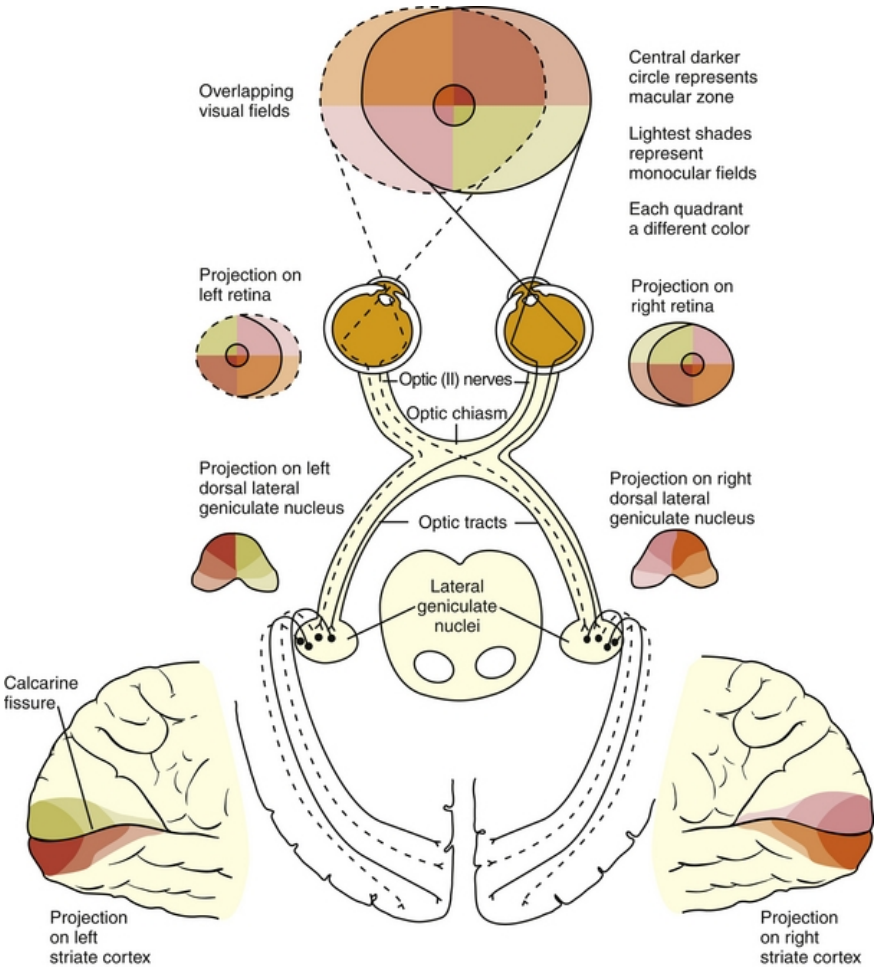

Figure 1.1 – Diagram of the visual pathway (*Source: https://basicmedicalkey.com/*).

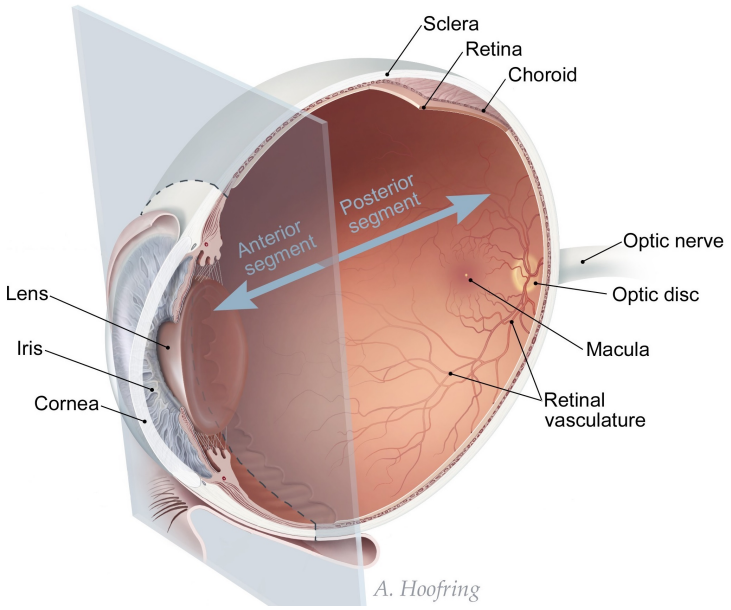

Figure 1.2 – Eye structure diagram (*Source: NIH Medical Arts*).

1.3 From the optic nerve to the visual cortex

The optic nerve corresponds to the axons of the ganglion cells that constitute the last layer of the retina, which will be described in chapter 2. The two optic nerves then meet at the level of the optical chiasma which reconstructs the visual field and separates it into two parts. Indeed, the left part is treated by the right hemisphere of the visual cortex and vice versa (see Figure 1.1).

The continuation of the optic nerves after chiasma is called the optic tract. For each hemisphere, visual information is distributed to nuclei that have different roles. However, nearly 90% of the axons of the optic nerve move towards the lateral geniculate body of the thalamus.

Some examples among these nuclei:

- the lateral geniculate body (LGN). Located in the thalamus, it sends information that will be analyzed by the visual cortex;
- the suprachiasmatic nucleus (SCN). Located in the hypothalamus, this nucleus contains the biological clock allowing to synchronize the awakening/sleep cycle according to the presence or absence of light;
- the superior colliculus. Its role is to direct sensory receptors from the head to objects of interest.

Then, the nerve fibres that connect the lateral geniculate nucleus to the visual cortex are called optical radiations. An optical radiation lesion leads to partial or total loss of vision in the hemisphere concerned (anopia).

Finally, visual information is processed in the visual cortex which is the largest system in the human brain. It performs low level treatments (orientation, contours) but also high level treatments (shapes, movements).

Chapter 2

Anatomy and physiology of the retina

In this chapter, the main properties of the retina are summarized: its organization but also its signal processing within the visual system. In Section 2.1, an overview of its anatomical structure is given. And in Sections 2.2 and 2.3, we focus on the description of each type of retinal cells as well as their function.

2.1 The anatomical structure of the retina

The retina is the sensitive organ of vision and is located at the back of the eye attached to Retinal Pigment Epithelium (RPE) under the choroid. The retinal pigment epithelium is the pigmented cell layer that bring nutrients and oxygen from the choroid to the photoreceptor cells, and supplies, recycles, and detoxifies products involved with the phototransduction process. The choroid is the vascular layer of the eye filled with blood vessels that nourish the retina.

It has three specific areas (see Figure 1.2):

- the macula : central region of the retina, located close to the optical axis of the eye;
- The fovea : central region of the macula which corresponds to the highest density of cone-type photoreceptors. This is where visual acuity is at its peak;
- the optic disc : region of optic nerve emergence without photoreceptors.

The retina is a complex multi-layered structure that converts light into electrical signals and performs the first stages of image processing in vision. It is composed

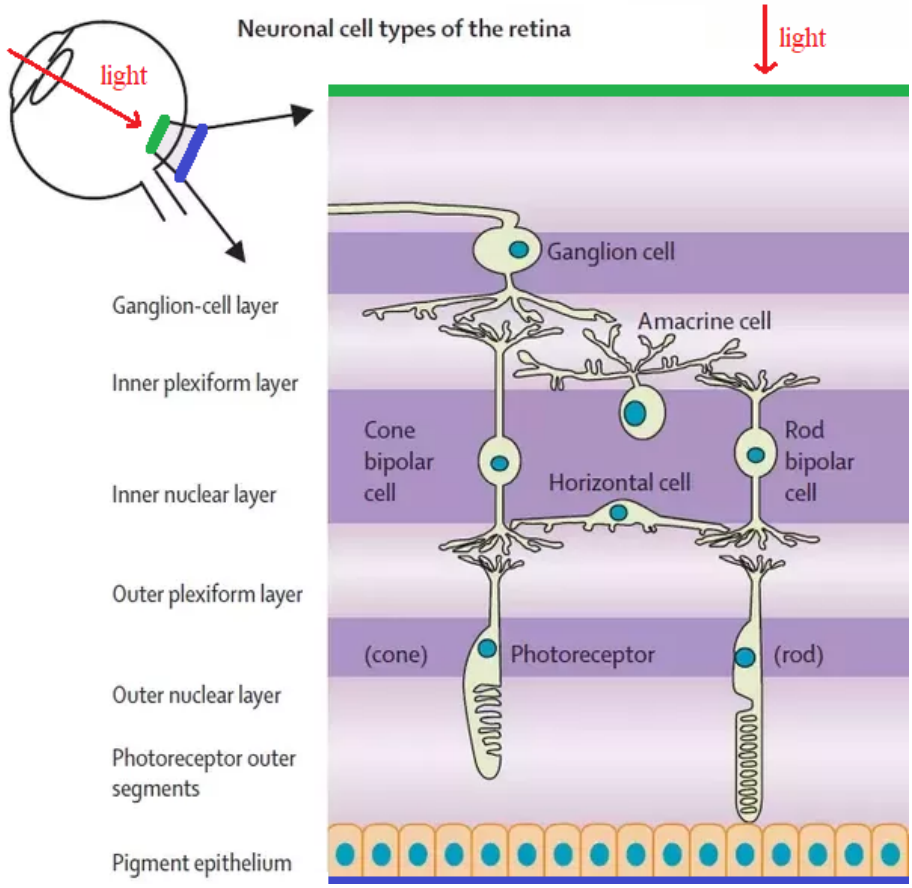

Figure 2.1 – Structure of the retina (Hartong et al. 2006).

of seven types of cells, three nuclear layers and two synaptic layers.

The nuclear layers are:

- the Outer nuclear layer (ONL) : photoreceptors (rods and cones);
- Inner nuclear layer (INL): horizontal cells, bipolar cells, amacrine cells;
- Ganglion cell layer (GCL) : ganglion cells (output cells, axons form the optic nerve), displaced amacrine cells;
- The retina is also composed of Müller cells (type of glial cells) that ensure both homeostasis (the tendency of organisms to regulate themselves and maintain their internal environment in a stable state) of tissues and the protection of neurons.

The synaptic layers are:

- Outer plexiform layer (OPL) : synaptic contacts between photoreceptors, horizontal and bipolar cells;

- Inner plexiform layer (IPL) : synaptic connections between bipolar, amacrine and ganglion cells. IPL is divided into On and Off layer.

2.2 Feedforward connectivity

2.2.1 Photoreceptors

In the retina, only photoreceptors are sensitive to light. There are three types of them:

- The rods: about 120 million in the humain retina [9], they are located outside the foveal zone. Rods are low-light receptors responsible for scotopic (night) vision. They do not mediate color vision, and have a low spatial acuity;
- The cones: most of them are located in the fovea centralis, they are about 6 million in the human retina [9]. Cones high-light receptors responsible of photopic (daylight) vision. They ensure color vision and are responsible for high spatial acuity;
- The intrinsically photosensitive retinal ganglion cells (ipRGCs) are the third and rarest type of photoreceptor. Unlike the other two types of photoreceptors that show rapid hyperpolarization in response to a light stimulus, ipRGCs have a very slow response curve to light stimuli, allowing them to integrate information over a long period of time. Their role is therefore more dedicated to reporting the overall level of light intensity rather than transmitting detailed information about the visual image.

2.2.2 Phototransduction

The retina has the capacity of converting photons in variations of electric potential. Phototransduction provides an enormous signal amplification system and consists of several stages:

- A photon is captured by a visual pigment molecule, called opsins (rhodopsins in the case of the rods);
- The activation of a molecule induces a cascade of chemical reactions whose multiplicative factor is huge. Indeed, for one activated rhodopsin molecule, there are 800 transducin molecules and 4 800 activated cGMP molecules participating to the enzyme cascade;

- It then causes the closure of 200 Na+ channels (representing 2% of all channels of a rod) that induces a significant variation of the photoreceptor membrane potential.

Therefore, to sum up, one single photon triggers a variation of 1mV in the photoreception membrane.

It is interesting to do an analogy between phototransduction (biological system) and photomultiplier (electronic system). The photomultiplier is a photon detection device in the form of an electron tube containing a photocathode, several dynodes (electrodes) and an anode. Under the action of light, electrons are ejected from the photocathode by photoelectric effect followed by a multiplier effect.These detectors multiply the current produced by incident light by as much as 100 million times. However, unlike the biological system, this one requires a greater consumption of energy to impose the tensions of the various components. Indeed, each dynode is held at a more positive potential (by about 100 Volts) than the preceding one.

In contrast, photoreceptors, and more generally retinal cells, handle voltages of order mV and currents of nA.

2.2.3 Bipolar cells

Bipolar cells are so-named because they have a central body with two extensions (axons). They transmit signals from photoreceptors or horizontal cells directly or indirectly to ganglion cells (via amacrine cells).

A bipolar cell is synaptically connected to nearly 100 photoreceptors grasping the light from a local region of a visual scene. As a consequence, the bipolar cell will respond electrically (variation of its membrane potential) to the light pattern occuring in this region. This leads to the notion of receptive fields explained in Figure 2.2.

Moreover, unlike most neurons, bipolar cells communicate through graduated potentials, rather than action potentials. Depending on the stimulus, the graduated potentials can be depolarizing (OFF) or hyperpolarizing (ON), while the action potentials always lead to depolarization of the membrane and inversion of the membrane potential.

2.2.4 Ganglion cells

Retinal Ganglion Cells (RGC) are at the final stage of retina encoding. They are the ones that emit spikes (via their axons which constitute the optic nerve) to the visual cortex, via the thalamus (LGN). Spikes consist of stereotyped mechanism which is

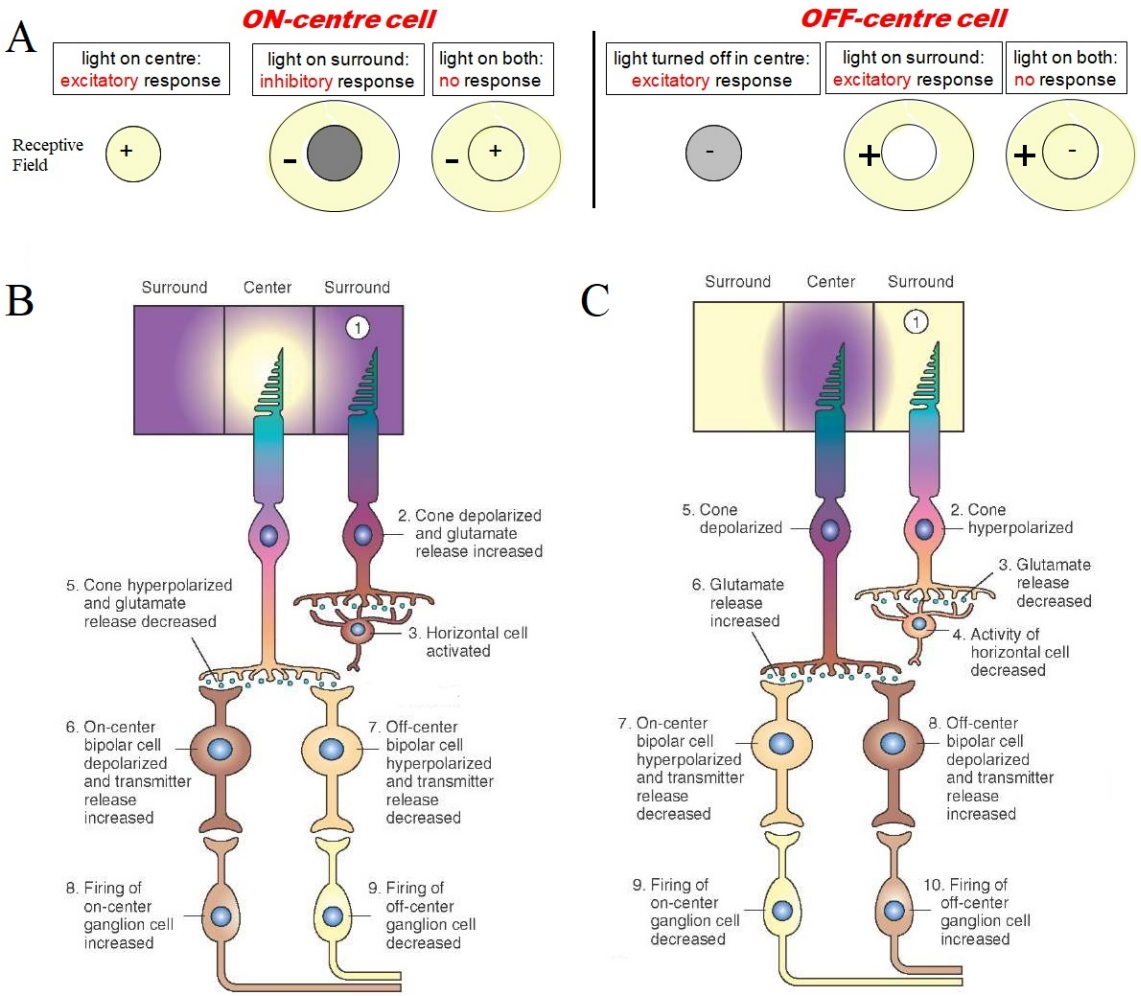

Figure 2.2 – Responses of retinal bipolar and ganglion cells to darkness and illumination in centre-surround receptive fields (*Source: http://what-when-how.com/neuroscience/*). (A) ON and OFF type center-surround cells (*Source: Evelyne Sernagor, lecture on the retina, september 2015*). (B) Changes in the electrical activity of the photoreceptor and on-center and off-center bipolar and ganglion cells when the photoreceptor receptive field surround is in the dark. (C) Changes in the electrical activity of the photoreceptor and on-center and off-center bipolar and ganglion cells when the photoreceptor receptive field surround is illuminated.

initiated by excitatory presynaptic potentials, causing the membrane potential to rapidly increased and then decrease. There are about 1.2 to 1.5 million retinal ganglion cells in the human retina. With about 125 million photoreceptors per retina, on average each retinal ganglion cell receives inputs via bipolar cells from about 100 rods and cones. However, these numbers vary greatly among individuals and as a function of retinal location. In the fovea, a single ganglion cell communicate with a few number of photoreceptors, while in the extreme periphery, a single ganglion cell receive information from many thousands of photoreceptors. Like bipolar cells, RGN can also be of ON of OFF type. They are also diversified in terms of receptive fields (notion described in Figure 2.2) which can be roughly divided in 3 groups:

- Magnocellular (M-retinal ganglion cells) have relatively large center-surround receptive fields, are color insensitive, and are most sensitive to movement of visual stimuli;
- Parvocellular (P-retinal ganglion cells) have relatively small center-surround receptive fields, are color sensitive, and are well suited for detecting contrasts that form the basis for shape discrimination;
- Koniocellular behave like P-retinal ganglion cells, have the smallest concentric receptive fields, have stronger color sensitivity than P-retinal ganglion cells, and are well suited for detecting colors that aid in shape discrimination.

2.3 Lateral connectivity

2.3.1 Horizontal cells

The horizontal cells are laterally connected to several cones, rods and bipolar neurons. Their role is to inhibit the activity of surrounding cells. This selective suppression of certain nerve signals is called lateral inhibition and its general role is to increase the acuity of a sensory signal by suppressing the signal of less illuminated photoreceptors.

It results in the center-surround architecture presented in Figure 2.2: When the centre field of a bipolar cell is illuminated, there is a hyperpolarization of center photoreceptors. Less illuminated photoreceptors in the surround field cause the hyperpolarization of horizontal cells, which by releasing neurotransmitters [1] trigger the depolarization of the surround photoreceptors.

[1] As a reminder, neurotransmitters are chemical messengers that transmits signals across a chemical synapse from one neuron to another.

2.3.2 Amacrine cells

The morphology of amacrine cells is very diverse and they use an impressive number of neurotransmitters. Their cellular bodies are all located in the inner nuclear layer (INL) and their synaptic endings in the inner plexiform layer (IPL). By connecting bipolar and ganglionic neurons, they form an indirect alternative route between them. Amacrine cells seem to have many functions, most of which are still unknown, but some specific functions can be outlined [4]:

- Form an indirect alternative route between retinal ganglion cells and bipolar cells in the IPL;
- Create functional subunits within the receptive fields of many ganglion cells;
- Contribute to vertical communication within the retinal layers;
- Through their connections with other retinal cells at synapses and release of neurotransmitters, they contribute to the detection of directional motion. They also modulate light adaptation and circadian rhythm, and control high sensitivity in scotopic vision through connections with rod and cone bipolar cells;
- They also contribute to differential motion detection.

Chapter 3

Retinal degeneration and treatments

3.1 Retinal diseases

There are many retinal diseases that can affect any part of the retina, and most of them cause visual symptoms. If left untreated, some retinal diseases can cause severe vision loss or blindness. Depending on the disease and the patient's condition, there are treatments that aim to stop or slow the disease or even partially restore vision. We will focus here on diseases that have received treatment in terms of gene therapy, cell transplantation and retinal prostheses.

3.1.1 Retinal degeneration (rhodopsin mutation)

Retinal degeneration is the deterioration of the retina caused by the progressive and eventual death of the cells in the retina. People with retinal degeneration may have the following symptoms: visual impairment such as the development of black spots in the field of vision for example, night blindness, retinal detachment, sensitivity to light, tunnel vision and loss of peripheral vision until complete loss of vision.

3.1.2 Retinitis Pigmentosa (rod-cones distrophy)

Among degenerative diseases of the retina, retinitis pigmentosa (RP) is one of the most common diseases. RP is a group of hereditary diseases that cause retinal degeneration. In most cases, the rods are affected first, affecting peripheral and night vision. As the disease progresses and the cones are affected, there is a decrease in visual acuity, colour perception and central vision.

To be more precise, it is a disease that results from harmful changes in genes that carry the instructions for making proteins that are needed in photoreceptors. Three scenarios can result in damage to photoreceptors [4]:

Figure 3.1 – Visual perception of a person with retinitis pigmentosa.

- The cell's functioning is limited by the severity of gene mutations that cannot then produce the required protein;
- Some mutations produce a protein that is toxic to the cell.;
- Finally, other mutations lead to an abnormal protein that does not function properly.

3.1.3 Macular degeneration

Also called Age-related Macular Degeneration (AMD), it affects older people and results in the distortion and loss of vision in the center of the visual field (see Figure 3.2). In the Western world where population is aged, it is the most common retinal disease because it is the leading cause of blindness and visual impairment in the elderly [4].

It occurs in two forms:

- In the "dry" form, there is gradual degradation of the photosensitive cells in the macula and the supporting tissue under the macula. These changes cause vision loss at several points in the center of the visual field;
- In the "wet" form, abnormal blood vessels grow underneath the retina. These vessels can leak fluid and blood, which can cause swelling and damage to the macula. Unlike the dry macular degeneration, damage can be rapid and severe.

While this disease does not lead to total blindness, it does result in distorted vision with loss of contrast sensitivity. For example, a grid of straight lines appears wavy at its center; contours are less sharp and shadows and colors less vivid (Figure 3.2).

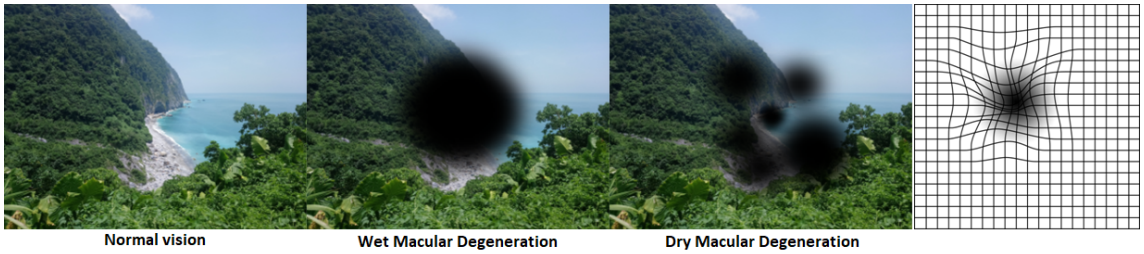

Figure 3.2 – Visual perception of a person with macular degeneration. And visual perception of a grid (*Source: https://www.allaboutvision.com/conditions/amd.htm*).

3.2 Retinal therapy

Today, retinal therapies are essential to stop retinal diseases and even partially restore vision to near-normal acuity. Currently, techniques such as electrical prostheses, for instance, make it possible to partially restore sight to blind people. The patient can then read large letters or catch objects. Their daily lives are therefore greatly improved, for example by being able to move around or climb stairs.

3.2.1 Genes therapy and stem cells transplant

Gene and cell therapies have the potential to prevent, halt, or reverse diseases of the retina in patients with currently incurable blinding conditions.

The gene therapy apply only for very specific diseases involving a few genes mutations. Its goal is to virally supplement retinal cells expressing mutant genes with healthy forms of the gene. It thus allows the repair and proper functioning of retinal photoreceptor cells in response to the instructions associated with the healthy gene inserted via a virus vector (tools commonly used by molecular biologists to deliver genetic material into cells [Wikipédia]). Likely, gene therapy may preserve remaining healthy retinal cells but it fails to repair the damage in already diseased photoreceptor cells [4].

For its part, stem cells transplantation is currently investigated with the objective of repairing the damage caused by the loss of photoreceptors. Since the inner part of the retina is left intact by the photoreceptors degenereration, replacement by stem cell could be efficient. Indeed, to contribute to the retinotopic map, the new cells need to make the right synaptic connections with the inner layer of the retina.

3.2.2 Retinal protheses

Even if retinal degenerative diseases leave the retina unable to sense light, there are still neurons remaining in the retina (bipolar and ganglion cells) that can be

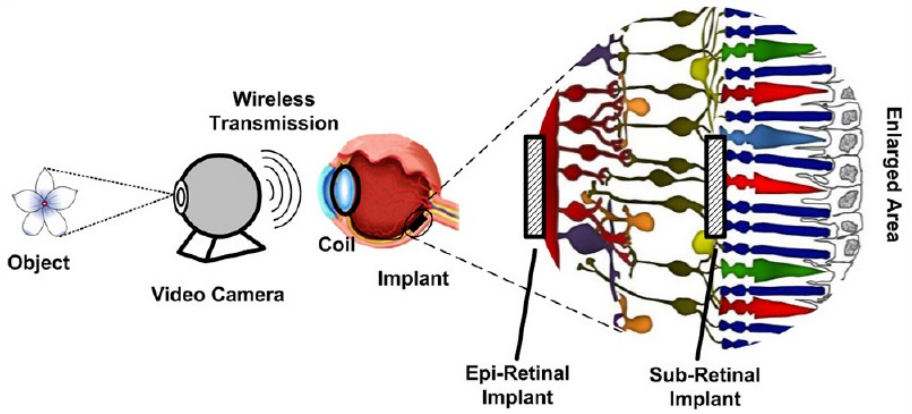

Figure 3.3 – Chain of function of retinal prostheses. Two types of retinal electrical implant (epiretinal or subretinal) are shown on the enlarged area (*Source: Journal of ophthalmic & vision research website*)

electrically activated on the base of established techniques for nerve stimulation.

For this, there are currently two types of retinal prostheses: electrical and optogenetic protheses.

3.2.3 Optogenetic prostheses

These new generation prostheses are based on the photosensitization of neurons ([4], Wikipédia). In other words, it involves genetic modification of nerve cells so that they become sensitive to certain wavelengths. Photosensitization is obtained by injecting a viral vector allowing the production of specific cells in a target zone of the retina. This method is very recent and is still under development (first human trial in 2016), but it is expected to restore vision to near normal acuity.

3.2.4 Electrical protheses

The retinal prosthesis is composed of three elements (see Figure 3.3): a camera that converts photons into digital data, an electronic microcircuit (which transforms the camera information into an electrical signal and produces stimulus current) and a matrix of microscopic electrodes (implanted in the eye in contact with the retina, it directly delivers coded information to the inner layers of the retina).

As a reminder, when the photoreceptors of the retina are defective or even inoperative, the biochemical processes that convert photons into action potentials are no longer effective. The purpose of implanting an electrical prosthesis is therefore to replace these chemical processes and directly send coded information to the inner layers of the retina, by electrically stimulating ganglions cells.

There are two types of electrical prostheses: epiretinal or subretinal implants.

Note however that it is the electrons that carry the charge in the metals, whereas in the body, it is the ions. In addition, living systems have been able to perform highly sophisticated cognitive tasks with minimal energy consumption, unlike electronic systems. Indeed, even if each unit works slowly, the whole system is massively parallel.

The difference in the nature of these two components imposes two problems :

- The Joule effect: The implantation of a prosthesis must necessarily take into account this very restrictive effect. The amount of information sent cannot be too significant due to heating of the electrode, which may burn the eye or cause pain. The dangerous effects of a rise in temperature imposed by the Joule effect limit therefore the sending of information;

- The electronic prosthese and the retina are not perfectly touching each other. The aqueous system at the back of the eye forms an interface between the two systems, which causes the electrical signal to diffuse.

Electrical prostheses have several additional limitation such as:

- the electrodes are larger than the retinal cells, making it difficult to target individual cells;

- Electrical stimulus can excite but not inhibit neurons;

- Since electronic retinal prostheses are implanted, the device lifespan must be as long as possible while ensuring that they do not cause functional loss to surrounding tissues.

Finally, although retinal prostheses have many limitations, they still make partial vision restoration possible in blind people which is an important progress. They can read big letters, catch objects and even climb stairs. However, this technology is still poorly mastered and only a few companies are manufacturing retinal implant, such as the French company Pixium Vision and the American company Second Sight Medical Products.

Chapter 4

Physiological model of the neural processing of visual information

The visual cortex, mainly occupying the occipital lobe of the brain, is responsible for processing visual information.

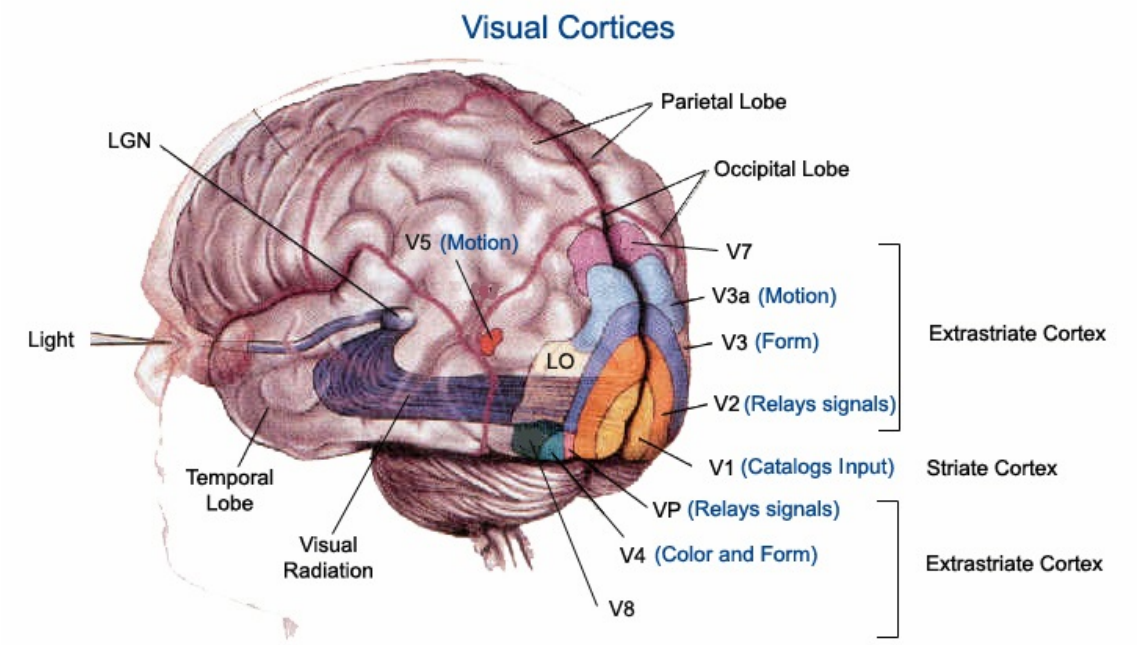

Figure 4.1 – Diagram of the visual cortices (*Source: http://www.galileiani.it/rubriche-galileiane/ma-cosa-sogna-un-cieco-e-un-feto/*).

Among the visual areas we distinguish:

- the primary visual cortex or area V1 which is the best understood part of the visual cortex and the part on which our model will focus;
- the extrastriate areas which correspond to all visual areas other than V1 (i.e. V2, V3, VP, V4, MT...).

4.1 The visual cortices

The visual cortex is divided into 5 distinct zones, V1-V5.

The primary visual cortex or V1 is the first to receive and process information. Its specificity is to process information about static and moving objects, but also in pattern recognition.

After a first processing in this area, the visual neural spikes are directed towards the secondary visual cortex or V2, which performs further interpretation. V2 then projects itself towards the other zones which make it possible to identify the colours (V4), the movement (V3a and V5), the forms (V3 and V4), etc.

Each of these areas is subdivided and constantly and simultaneously exchanges messages with at least 20 other areas of the brain that process visual information. It is this massively parallel processing that allows a global visual perception of our environment.

4.2 Retinotopy

Retinotopy refers to the spatial organization of neural responses in V1 to visual stimuli. In other words, it is a bijective correspondence between an illuminated area of the retina and an area of neurons in the cortex; it is a mapping of the retina in the cortex.

This mapping is however very difficult to express in an analytical way for the following reasons [6]:

- It is non-linear;
- Because the retina is a hemispheric plane, it is expressed from polar coordinates;
- It varies from one animal to another.

In order to obtain a mapping of the retina, different areas of the visual field are illuminated one after the other. The observation by optical imaging of the activated area in the cortex then indicates the position of the corresponding zones.

Scientists are therefore led to extrapolate experimental results in order to obtain a model of the retinotopy, by averaging the maps obtained for a set of animals.

Studies on the retinotopies of the rat [3] and of the monkey ([6],[2]) proved how different visual perception can be between two animals.

Retinotopy of the rat

The analytical form of the retinotopic map is not known for the rat. Thus, F. Chavane and S. Roux used the same methodology as [3] to express the retinotopic map. Because of its complexity, two simplifications were then made:

- Since the rat has no fovea, the cortical position is determined by the distance of the point in the retina from the optic disc;
- In order to simplify the numerical calculations, Frédéric Chavane's model uses cartesian coordinates. The coordinates of the cortical position can be determined independently according to decreasing functions of the form $\frac{1}{ax+b}$ and $\frac{1}{cy+d}$, with x and y the horizontal and vertical distances from the optic disc.

The experiment is conducted by splitting the left rat's visual field into several zones (Figure 4.2A). Each area is then illuminated to observe the associated cortical activity in the right hemisphere of the visual cortex. A mapping of the retina in the visual cortex is then obtained by averaging data from several rats (Figure 4.2B).

It should be noted that these experiments are complex to set up [3] because it requires surgery. A median incision is made to expose the surface of the skull. A part of the skull covering the right primary visual cortex is then thinned to translucent. Performing this procedure instead of a craniotomy (surgical operation in which a bone flap is temporarily removed from the skull to access the brain [Wikipedia]) provides sufficient image quality while preserving the integrity of the intracranial environment.

In addition, the experiments are conducted on several rats, which requires a certain amount of preparation and measurement time.

Retinotopy of the monkey

Preliminary studies were conducted on rats. However, retinal prostheses are a priori implanted in humans. The interest is now to understand the diffusion effects (subsection 5.2.1) in animals closer to humans.

Knowing that the speciality of INT Marseille, in particular of F. Chavane, is to work on non-human primates, the next step consists in carrying out the same experiments in the case of the monkey.

The model done for the rat must therefore be adapted to extend the results to non-human primates or retinal degeneration models in order to better understand the retinal diseases in humans. Since rats do not have a fovea, their retinotopy was

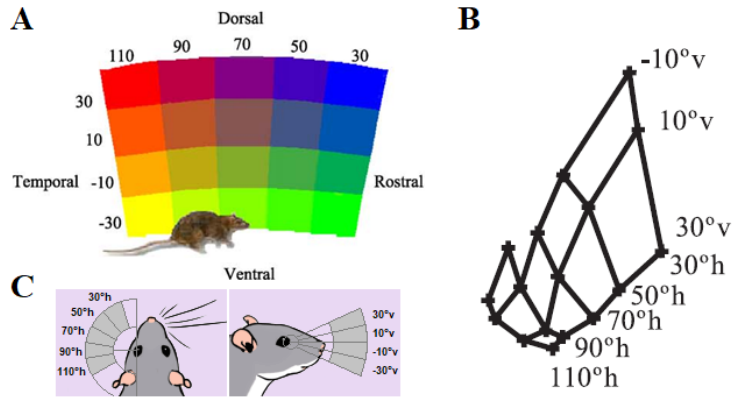

Figure 4.2 – (A) Color code of the visual field location of the stimuli [3]. (B) Representation of the rat visual field projection and the centres of activity onto primary visual cortex according to the average retinotopic map across rats [3]. (C) This figure, from my own, shows the representation as I understood it of the visual field on which the light stimuli will appear

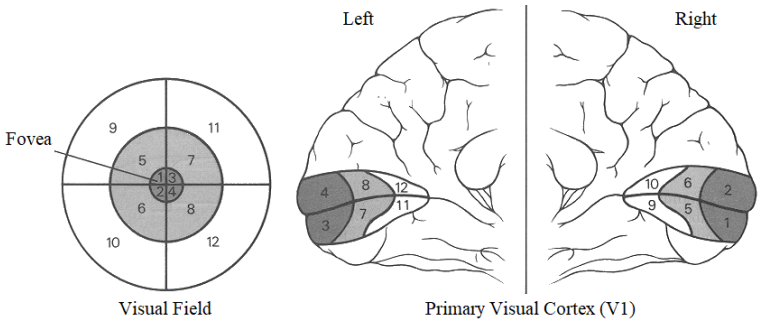

Figure 4.3 – Representation of the visual field and the respective areas in the V1 cortex for the monkey. Information from the left visual field is processed by the right hemisphere of the visual cortex, and vice versa (*Source: fourier.eng.hmc.edu*).

calculated according to the distance to the optic disc. Therefore, the model must be modified to take into account the existence of fovea in primates.

Because it is the area of the retina with the highest concentration of photoreceptors, the foveal area is more represented in V1 than the peripheral areas.

Retinotopy in primates has an elliptic shape with one end corresponding to the fovea and the other to the far periphery.

Note on Figure 4.3 that the central 5 degrees in the monkey visual field represents about 40% of the cortex. This disproportion between the central and peripheral areas is referred to as cortical magnification.

[6] (whose work was used and confirmed by [2]) showed that it was possible to determine the retinotopy of a monkey after calculating three parameters intrinsic to the animal (k, a and α). The map of the visual space in V1, symbolized by the function w, is defined by the following :

$$w(E, P) = k \times log(E \times e^{iPf_a} + a) \tag{4.1}$$

$$\text{where} \begin{cases} E & \text{is the retinal eccentricity} \\ P(\theta) = \alpha \times \theta & \text{is the angular deviation from the horizontal meridian} \\ f_a(E,P) = sech(P)^{sech(\log E/a \times 0.76) \times 0.1821} & \text{is a shear function.} \end{cases}$$

with:

- θ : the original polar angle
- α : a compression parameter reflecting the angular compression along the iso-eccentricity curves
- k : a scaling constant
- a : a structural parameter that defines the limit of the foveal singularity

4.3 The importance of "reciprocal" connections between areas of the visual cortex

Optical illusions are an effective way to prove the complexity of the visual system. When processing visual information, there may be conflict between cells that respond to the same stimuli (e.g. contours) but with different abilities. The reciprocal connections that allow information to flow in both directions between different areas of the visual cortex are then essential. An example of this type of conflict is given by the Kanizsa triangle.

In this visual illusion, a normal observer perceives a white triangle superimposed on a triangle with a black outline. It has been shown (von der Heydt and Peterhans 1989) that shape-sensitive cells of the V1 area do not react when looking at the figure and do not detect the absent line. This is because the majority of cells in V1 are simple cells with a single receptive field. In contrast, the cells in area V2 are more complex because they respond to the summation of several receptive fields which are integrated from many simple cells [11]. So, even though V1 and V2 cells respond to the same visual cues such as the orientation of edges and lines, they will not give the same interpretation of the same information.

For the Kanizsa triangle, V2 cells interpretation infer the presence of a "line" instead of the non-existent white contour. There is then harmonization of the results of the treatments carried out by the two areas thanks to the reciprocal connections

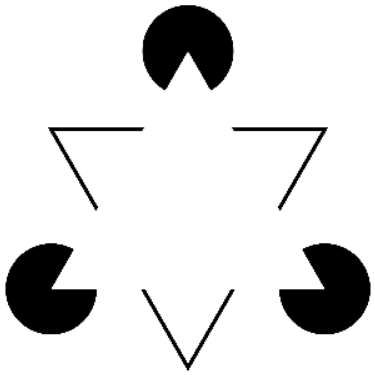

Figure 4.4 – The optical illusion of the Kanizsa triangle [Wikipedia].

between them, which makes it possible to carry out a visual construction of the two triangles.

Part II

Study topic and description of the model

Chapter 5

Study project

Recent advances in neuroscience and microelectronics offer the prospect of partially restoring the vision of blind patients using retinal prostheses (chapter 3). However, because this area of research is at an early stage, devices have several limitations and some main concepts are still not well known. Especially, the way an electric stimulation activates the visual cortex is poorly understood.

5.1 State of the art

Equipped with retinal implants, patients - totally blind - recover visual perceptions in the form of phosphenes. At present, unfortunately, the perceived light signals are not accurate enough to restore a sufficient level of vision so that they have a minimum of autonomy on a daily basis.

In order to understand the resolution limits of the image generated by the prosthesis, a vast experiment on the rat was conducted at INT Marseille by F. Chavane's team. The objective of this study was to compare the visual system response of a rodent with natural visual stimuli and stimuli produced by the prosthesis, with the aim of optimizing retinal implants.

For the experimentation [1], F. Chavane et al. used subretinal Micro Electrode Arrays (MEAs) manufactured at the CEA-LETI (Pham et al., 2013) (Grenoble, France). These planar MEAs of 1 and 1.2 mm diameter comprise respectively 9 and 17 (50 μm radius) electrodes. As for the model, we assumed that an implant size 30 would represent a whole MEA stimulation (wMEA), and an implant size 5 would represent a single electrode stimulation (SE).

The results show that V1 is activated at the appropriate position and with amplitudes comparable to those obtained under natural conditions. Unfortunately, the activation zones are too large and too elongated compared to the result obtained for

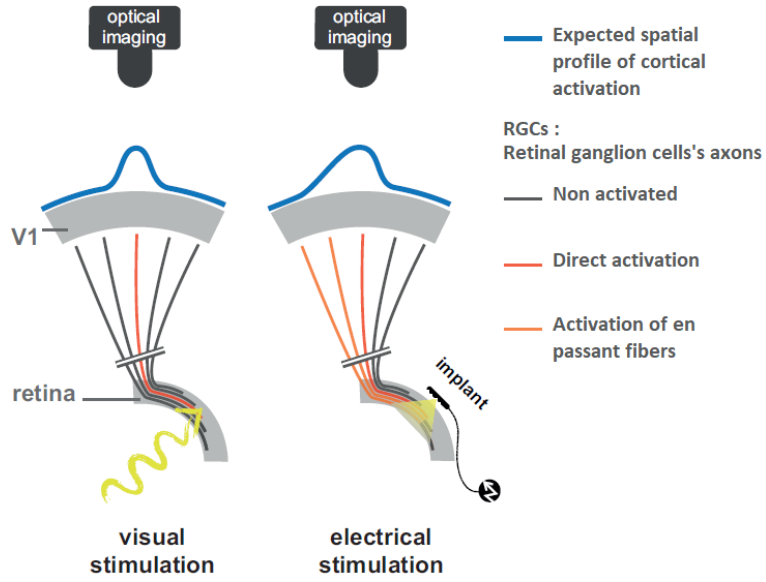

Figure 5.1 – Schematic view of the experimental setup with the camera and the visual pathway from the retina to V1 activated with normal visual stimuli (left) or with sub-retinal electrical stimulation using a MEA (right). *Source: [1].*

a visual stimulus.

This deformation may be due to the four diffusion phenomena described in the next Section. The interest of a better knowledge of the intensity of influence of each parameter is to offer the necessary material to optimize retinal implants.

5.2 A model of retino-cortical activation by electric stimulation

5.2.1 Effects to consider

Four effects may be responsible for the extent of artificially evoked cortical activity:

- 1) an electric diffusion at the interface made by the complex electrode-retinal tissue;
- 2) an electric diffusion in the visual cortex;
- 3) the optical diffusion of the signal registered by optical imaging;
- 4) a spread of electric activity induced by the direct activation of retinal cells axons away from their somata (see Figure 5.1).

If the first three effects can be described by standard diffusion equations, the effect due to axons "en passant" activation is asymmetric and complex. The different

intensities of these effects should also be taken into account in order to provide a reliable model.

As shown in Figure 5.1, the cortical profile is symmetric for visual stimulation and asymmetric for electrical stimulation if axons "en passant" are activated.

5.2.2 Steps and characteristics of the simulation model

In [1], a 2D simulation model of cortical activity evoked by artificial retinal implants was implemented by F. Chavane and his collaborators. The final objective of this modeling is to be able to characterise each diffusive effect independently. This will then make it possible to estimate the intensity of each of them by comparing the experimental results with those obtained for a set of parameters.

First step - Model of the retinal activation

A functional model was designed to predict the spatial characteristics of retinal activation triggered by electrical stimulation. The retinal plane is represented by a two-dimensional matrix of dimension N:

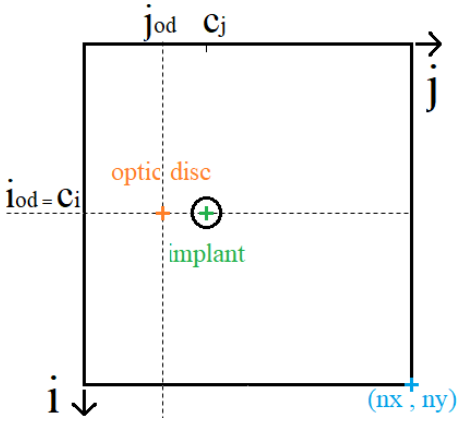

Diagram of the matrix representing the retinal plane.

To predict the profile of retinal activation (its level, shape and size), two activity diffusion components, that extend beyond the electrode surface, were introduced:

- An isotropic Gaussian diffusion (G): corresponding to the second effect presented in subsection 5.2.1;
- A diffusion due to the passing activation (EP) of ganglion cell axons;
- These diffusions are calculated in response to a stimulation of a given size and location in the retinal space.

The first contribution to retinal activation is the isotropic 'direct' activation induced by implant stimulation which was modeled as a 'flat-top' Gaussian that can be expressed as follows:

$$IsoA(i,j) = \begin{cases} 1, \quad \text{if} \quad \sqrt{(i-c_i)^2 + (j-c_j)^2} < s_z \\ e^{-\dfrac{(i-c_i)^2 + (j-c_j)^2}{2 \times (\sigma \times s_z)^2}}, \quad \text{if} \quad \sqrt{(i-c_i)^2 + (j-c_j)^2} \geqslant s_z, \end{cases} \tag{5.1}$$

Where (i,j) and (c_i,c_j) are the position in space and the position of the implant respectively, s_z the size of the electrode and σ the spatial isotropic diffusion extending beyond the electrode.

The other contribution to retinal activation is anisotropic "en passant" recruitment of ganglion cell axons. It was modeled as a shadow cone activation that results from the isotropic "direct" activation. Its expression is the following:

$$EP(i,j) = Att(i,j) \times Sig(i,j) \times Cone(i,j) \tag{5.2}$$

As written, its computation results from the multiplication of three functions:

- *Cone* : cone-like activation modeled as an angular Gaussian activation. It represents the exponential decay of the quantitity of activated ganglion axons "en passant" as a function of the angle to the horizontal axis (maximum horizontally);
- *Sig* : sigmoid function centered on the position of the optic disc;
- *Att*: general attenuation of the activation centered on the position of the implant.

Their expressions have been obtained empirically:

$$\begin{cases} Att(i,j) = e^{-\dfrac{\left(\sqrt{(i-c_i)^2 + (j-c_j)^2} - s_z\right)^2}{2(N/2)^2}} \\ Sig(i,j) = \dfrac{1}{1 + \dfrac{dOD - (c_j - j_{od})}{s_z/4}} \\ Cone(i,j) = e^{-\dfrac{ConeAng^2}{2 \times \sigma^2}}, \quad \text{if} \quad j > j_{od} \end{cases} \tag{5.3}$$

With

- N is the size of the matrix representing the retinal plane;
- (i_{od}, j_{od}) is the position of the optic disk;
- $dOD(i,j) = \sqrt{(i - i_{od})^2 + (j - j_{od})^2}$ is the distance to the optic disk;
- $ConeAng = |atan2(i - iod, j - jod)| / angleDisk$ is the normalized angle used in the calculation of the activation cone;
- $angleDisk = 2 \times asin(\frac{s_z/2}{dOD})$ is the angle formed by the tangents to the implant passing through the optic disc.

In the original model [1], the calculation of "angleDisk" was: $angleDisk = 2 * asin(s_z/dOD)$. However, as shown in Figure 5.2, the calculation must be done according to the radius and not the diameter of the implant. The computation (section 6.2) takes this change into account.

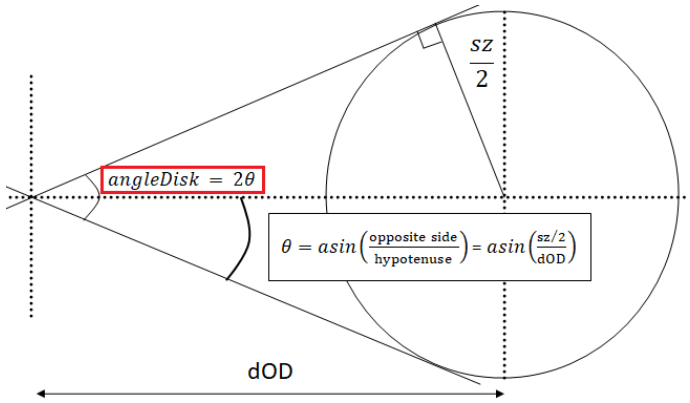

Figure 5.2 – Explanatory diagram of angleDisk calculation.

In our computation, $N = n_x = n_y$ is 400, σ is 1, (i_{od}, j_{od}) is (200,100), (c_i, c_j) is (200, 150), s_z varies between 3 and 30 pixels, and α between 0.1 and 1. Finally, these two activations (isotropic "direct" activation and anisotropic "en passant" recruitment of ganglion cell axons) are combined with different ratio α (contribution for the axons "en passant") via a weighted sum, :

$$retinian\_activation = IsoA + \alpha \times EP \tag{5.4}$$

Second step - Model of the cortical activation

Since the retinocortical transform has no analytical expression for the rat, F. Chavane and S. Roux had to determine its shape by experimentation. As a reminder, retinotopy is obtained by stimulating a set of areas of the retina until a map is

obtained in the visual cortex. By studying the data, they were able to define a bijective function whose form approximates the expected result.

This transform applies to the coordinates of a point independently according to the following expression:

$$RCT : \begin{cases} Retina \rightarrow Cortex \\ (i,j) \mapsto (\frac{1}{ai+b}, \frac{1}{cj+d}) \end{cases} \tag{5.5}$$

where a, b, c, d is the set of values selected by matching the function results with the rat retinotopy.

The implementation of this geometrical transform produces a correspondence between the coordinates of the retinal space and the cortical space. It remains then to interpolate the image representing the retinal activation.

Finally, the effects relative to the diffusion in the visual cortex and due to optical imaging do not have mathematical expressions. In the computation, they will be represented by a smoothing effect on the cortical activation.

Part III

Results

This part summarizes the work I did during my internship

The first step of the project was to reproduce the results obtained by F. Chavane et al. [1] to verify that the program was working properly.

The program is divided into two main parts, starting with the retinocortical activation model for a single set of parameters. This result in a set of the characteristics of the image region that define cortical activity (e.g. center of mass, aspect ratio, orientation).

The second part runs the model in a loop depending on the implant size and the α ratio (contribution of axons "en passant"). This allows us to find a correlation between the aspect ratio of evoked activations and the two parameters of the loop, which correspond to the diffusive effects 1 and 2 described in subsection 5.2.1.

After checking that the original program worked, the objective was to make changes. This consisted in the creation of functions as well as the questioning of some pieces of code.

Finally, I worked on the following two points:

- The determination of the parameters representing the four diffusion effects by fitting the model to the experimental data;
- Adapting the model to the monkey by implementing its retinotopy ([6], [2]).

Unfortunately I could not complete them due to lack of time.

Chapter 6

Replication of results from the original program and improvements that have been made

6.1 Familiarization with the program

The usual way to become familiar with a code is to first check that it is possible to execute it in its entirety, then read and display the figures as you go.

However, I decided to follow a different approach. In the code written by F. Chavane, many calculations were made in the main file. That's why I decided to familiarize myself with it by understanding and modifying one part at a time. I found that this approach allowed me to understand the code faster and get results more efficiently.

In addition to the creation of functions allowing the reduction of the main file, its syntax and readability have been simplified in order to lighten its reading. For example, any part of the code used to test functions or verify intermediate results has been moved to a test file. This file also contains all comparisons made between the original code and the results obtained from the so-called "reduced" code (which uses the newly created functions).

Finally, I also though that it was important to comment the code for potential future use. Therefore, in addition to the explanatory comments at the beginning of each function, each folder containing pdf files (containing questions and answers from conversations with F. Chavane), Matlab files or figures, includes a text file "Notes.txt". They give all the descriptions of the files found in the directory concerned (what each function is for, what the figures represent, etc). This synthesis, mainly for the description of the functions, helped me to take the file in hand.

6.2 The results of the model

6.2.1 For one set of parameters

The model was realized from a set of parameters giving (Figure 6.1:

- (nx, ny) : the size of the matrix representing the retinal plane;
- (i_{od}, j_{od}) : the position of the blind spot;
- (c_i, c_j, sz) : the position and the size of the implant;
- $baseline, amplitude, sigma, ...$: the parameters used to calculate the different diffusion effects (subsection 5.2.1). The use of these parameters will be given later.

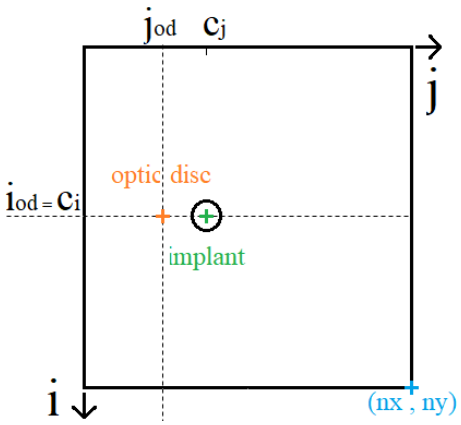

Figure 6.1 – Diagram of the matrix representing the retinal plane.

In our computation : $n_x = n_y = 400$, $(i_{od}, j_{od}) = (200, 100)$, $(c_i, c_j) = (200, 150)$ and $s_z = 30$.

For this whole part, the brightness codes the strength of the response, and all representations are scaled between 0 and 1.

Retinian activation profile

First, the retinian activation profile was create by implementation of the equations of section 5.2.2.

First, the isotropic "direct" activation is modeled by a flat-top Gaussian as shown in Figure 6.2. In order to do so, all points inside the implant were set as equal to 1, and beyond it follows a Gaussian attenuation.

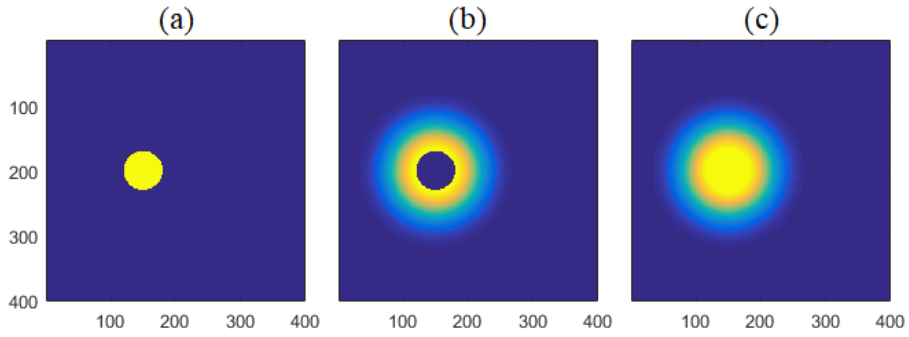

Figure 6.2 – Isotropic "direct" activation. (a) "Direct" activation from the implant. (b) Gaussian attenuation representing the electric diffusion at the interface made by the complex electrode-retinal tissue. (c) Sum of (a) and (b)

Then, the anisotropic "en passant" recruitment of ganglion cell axons was modeled as a shadow cone activation (see Figure 6.3). To do this, a multiplication was made between: .

- A Gaussian attenuation depending on the distance from the implant;
- A sigmoidal function: since the axons are oriented towards the optic disc, their activation by diffusion in the vicinity of the implant is only in the opposite direction. Indeed, the retina is organized in such a way that the axons of the ganglion cells furthest from the optic disc overlap those of the cells closer. This arrangement of axons, which can be considered in layers, is modelled by a sigmoid which is 0 between the optic disc and the implant, and which is 1 for a distance to the optic disc greater than that of the implant. In other words, the "direct" activation of the axons of the first layer will diffuse into the upper layers coming from areas further away from the optic disc;
- A Gaussian angular activation: Since the retinal plane is spherical and axons can be considered to move almost straight towards the optic disc, diffusion among axons has been modeled as a cone whose apex corresponds to the optic disc. For more simplicity, the angular distribution has been chosen Gaussian type even if it is not the only possible model (see section 6.4).

Note that the cone angle expression has been changed, from the one used in the original program to:

$$angleDisk = 2 * asin((s_z/2)/dOD) \tag{6.1}$$

The final step in that both activations are combined with different ratio α (contribution for the axons "en passant") via a weighted sum. Again, both profiles are shown depending on the calculation used for angleDisk (Figure 6.4).

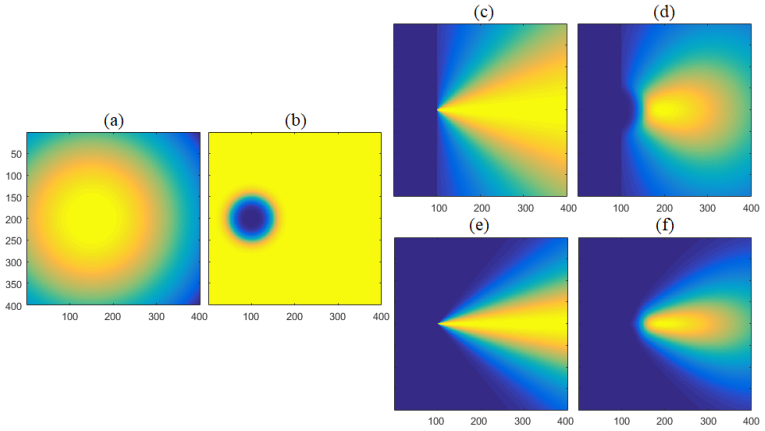

Figure 6.3 – Anisotropic "en passant" recruitment of ganglion cell axons. (a) Attenuation depending on the distance from the implant. (b) Sigmoidal function. (c,e) Gaussian angular activation. (d,f) Multiplication of the three components. (c,d) are the result obtained from the original angleDisk calculation, and (e,f) from the rectified calculation (Equation 6.1). We observe that they are different.

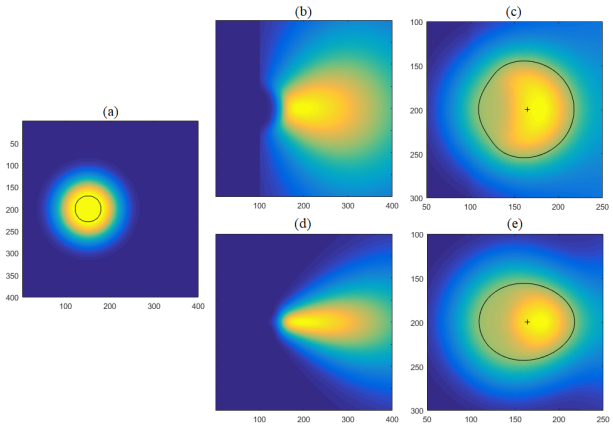

Figure 6.4 – Retinian activations. (a) Isotropic "direct" activation. (b,d) Anisotropic "en passant" recruitment of ganglion cell axons. (c,e) Retinian activations profiles. (b,c) are the result obtained from the original angleDisk calculation, and (d,e) from the rectified calculation (Equation 6.1). We observe that they are different.

In order to see the influence of implant size and of the contribution of axons "en passant", computation was done for two ratios (0.5 and 1) and three electrodes size (5, 15 and 30, rows).The retinian activations are shown in Figure 6.5.

Note that for the experimentation [1], F. Chavane et al. used subretinal Micro Electrode Arrays (MEAs) manufactured at the CEA-LETI (Pham et al., 2013) (Grenoble, France). These planar MEAs of 1 and 1.2 mm diameter comprise respectively 9 and 17 (50 μm radius) electrodes. As for the model, we assumed that an implant size 30 would represent a whole MEA stimulation (wMEA), and an implant size 5 would represent a single electrode stimulation (SE).

The importance of angle calculation is therefore obvious since the new cortical activation is more elongated that the result obtained with the original program.

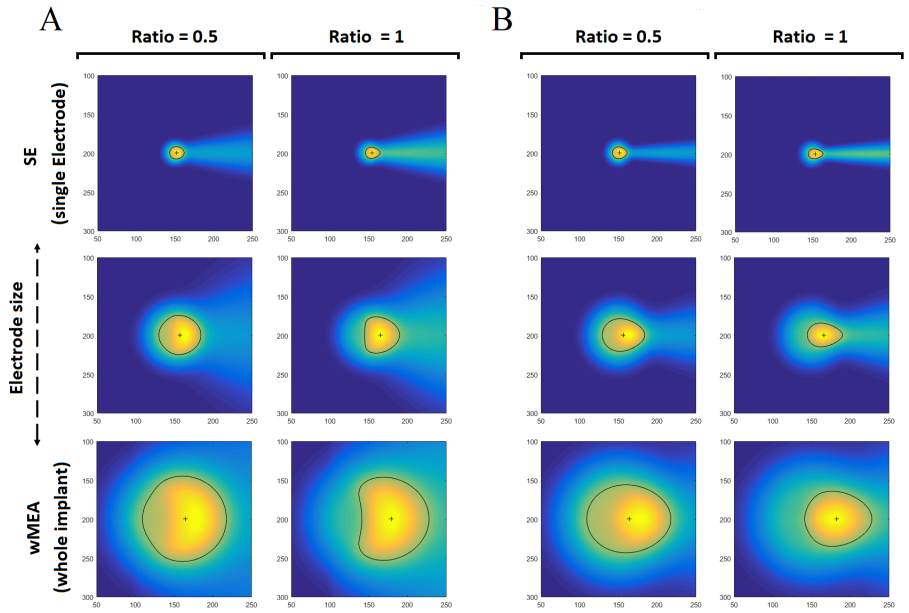

Figure 6.5 – Main steps of the computation depending on the implant size and the ratio of contribution axons "en passant". (A) Result obtained from the original angleDisk calculation. (B) Result obtained from the rectified calculation (Equation 6.1). Figure B shows that cortical activities are more elongated than those in Figure A (original results) which seems to correspond better to the observations made on the experimental data.

It remains to be determined which of the two angle expressions is closer to the biological system.

Finally, a smoothing was applied to obtain the retinal profiles. The relevance of using this smoothing criterion will be discussed in the section 6.5.

Cortical activation profile

In order to obtain the cortical profile, it is now necessary to implement Equation 5.5. For coordinates in the retinal space, this transform calculates the corresponding end point in the visual cortex. By performing the calculation on a certain number of points, it is then possible to obtain the cortical activation using two Matlab functions [5]:

- *"tform = fitgeotrans(movingPoints,fixedPoints,transformationType)* takes the pairs of control points, movingPoints and fixedPoints, and uses them to infer the geometric transformation specified by transformationType";
- "cortical_activation = imwarp(retinian_activation,tform) transforms the image retinian_activation according to the geometric transformation defined by tform, which is a geometric transformation object. cortical_activation is the transformed image".

Part of the program that could have been improved was to formalize the calculation of this transformation.

Since using the function *fitgeotrans* implies choosing among transformation types, i.e. interpolations, it causes inaccuracies.

Indeed, the transformation is done at the coordinate level. This means that the transform is applied to the coordinates in the plane of the retina in order to obtain all the arrival points. Since there is a distortion of the starting space in the arrival space, the "holes" created by this deformation need to be fill by interpolation. Hence, the interest of studying different possible types of interpolation in order to find the one that seems the most coherent.

The direct calculation of this transformation and the testing of different interpolations could thus give a more precise model of the result we want to obtain.

Unfortunately, I did not understand enough about interpolation, so I couldn't figure out how to implement it.

However, I did compare different types of transformation using the Matlab function (Figure 6.6):

- "polynomial : Use this transformation when objects in the image are curved". Among the orders I tried, 3 and 4 were the more accurate;
- "piecewise linear (pwl) : Use this transformation when parts of the image appear distorted differently". This is the type of transformation that was used in the original programme;
- "local weighted mean (lwm) : Use this transformation, when the distortion varies locally and piecewise linear is not sufficient".

The comparison of the cortical activations shows a very great similarity between 'pwl' and 'lwm' types (the forms seem equivalent and the regions eccentricities are equal). According to the definition of the "local weigh mean" transformation, it is deduced that the use of the "piecewise linear" type is sufficient.

On the other hand, the difference between the cortical profiles calculated from the polynomial transformations and the original result is visible. However, unlike order 4, the eccentricity region of order 3 is close to the value obtained by the other two transformations.

Nevertheless, only a formal calculation of the tranformation would make it possible to know if the use of the function *fitgeotrans* is sufficient or if it lacks precision.

Finally, it is reminded that rat retinotopy was obtained from experimental data. It would therefore be interesting to reproduce this test on an application whose mathematical form is known, such as the retinotopy of the monkey.

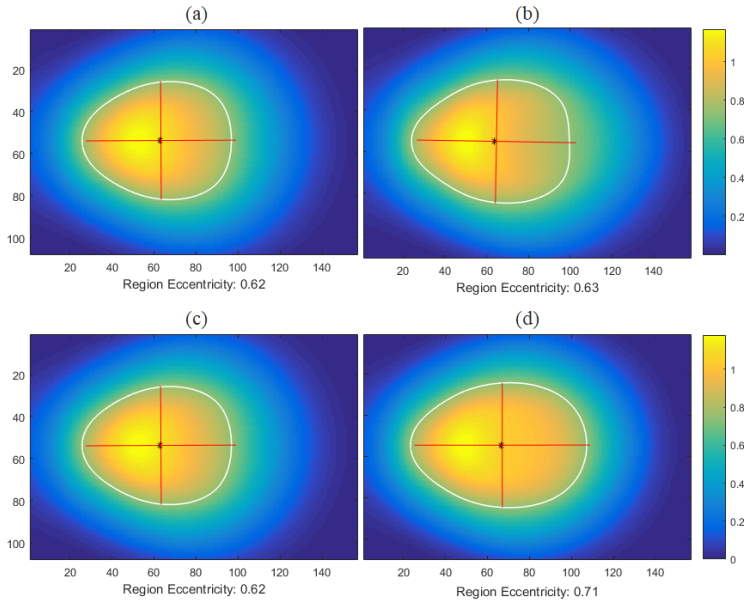

Figure 6.6 – Comparison between cortical activations depending on the type of transformation chosen when using *fitgeotrans*. (a) 'pwl'. (b) 'polynomial', order 3. (c) 'lwm'. (d) 'polynomial', order 4.

6.2.2 Examination of a multitude of cortical activities

By comparing cortical activations to visual and prosthetic stimuli from experimental data [1], an elongation of the profile for electrical stimulations was observed (Figure 6.7).

When compared to visual stimulus (white), the cortical activation for Single Electrode (Figure 6.7 blue) generally present an elongation that is not found in the case of a whole Micro Electrode Array (red) stimulation.

In order to quantify "the extent and the shape of the activation contour, we computed the equivalent ellipse (Haralock and Shapiro, 1991). This provides the length and orientation of the equivalent ellipse minor and major axes" [1]. The aspect ratios (AR between the major and minor axis) of activation contours were then calculated for different implant sizes and axons "en passant" contribution ratios.

The method revealed a correlation between these different characteristics. (see Figure 6.8A)

Figure 6.8 gives a prediction of the elongation of electrical activations as a function of the contribution of axons "en passant", the implant size and its distance to the optic disk.

The change of the cone angle expression for the calculation of the shadow cone activation (modeling the anisotropic "en passant" recruitment of ganglion cell axons) implies an important difference between the result obtained from the original program and the figure with rectified angle expression (Equation 6.1).

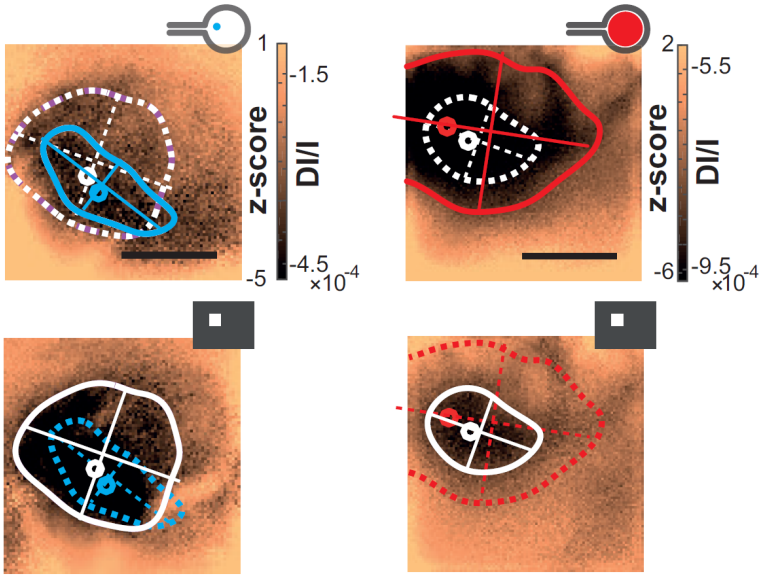

Figure 6.7 – [1] : "Shape of cortical activations generated in 2 animals by Single Electrode (blue) and by a whole Micro Electrode Array (red) stimulation at high current intensity (top) and their corresponding 20° visual stimulus (white, bottom)".

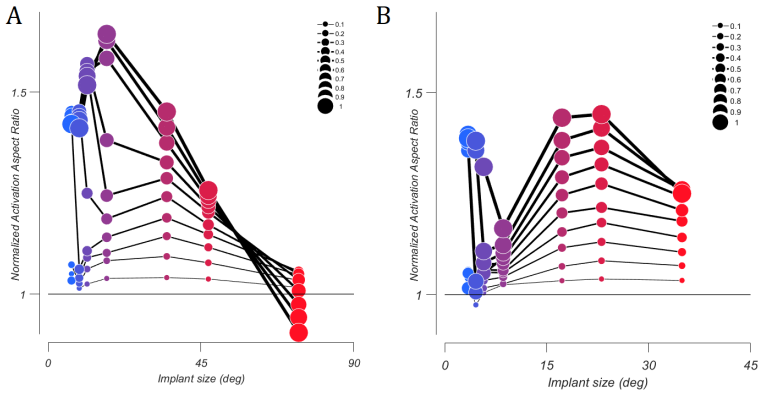

Figure 6.8 – Prediction of the elongation of electrical activations as a function of the contribution of axons "en passant", the implant size and its distance to the optic disk. The AR is Normalized ([1]: "Please note that, to account for any potential deformation of the evoked activity due to retino-cortical magnification factor or physiological noise, we normalized all electrically-induced AR"). (A) Original figure (Roux et al. 2012 - Figure 4C). (B) Figure corrected by taking into account the change in the expression of the implant angle (Equation 6.1).

However, the original figure seems to better match the experimental results. Indeed, for the smallest implant sizes, the AR is the highest, indicating an elongation in the case of SE stimulations. However, after correction of the expression of the implant size, the AR remains higher in the case of stimulation by wMEA, which does not correspond to the observations made on the experimental data.

Having only noticed very late that I had forgotten to change the expression of the angle in the calculations intervening in the loop, I did not have time to see with F. Chavane what he thought of this significant difference between the results of the model and the observations on the experimental data.

However, I think that the original version is closer to what I understood about the elongation of cortical activities.

6.3 The Naka-Rushton function [generalization of the sigmoidal function]

As described in the section 5.2.2, the activation due to the axons "en passant" is a multiplication of three components: an attenuation, a sigmoid function and an angular Gaussian activation.

The first change I made in the code was to generalize the sigmoid function used by a Naka-Rushton function.

I learned of the Naka-Rushton function when I read [1]. After some research, I found that it is defined as follows (*Naka and Rushton, 1966*):

$$Response : C \mapsto R_{max} \times \frac{C^n}{C^n + C_{50}^n} + b$$

with:

- b : the baseline (background discharge);
- R_{max} : the maximum response for a baseline of null value;
- C_{50} : the level of contrast which produces half of R_{max} (constant of semi-saturation);
- n: dimensionless constant that controls the slope of the curve at a contrast of C_{50}.

I then realized that any sigmoid function could be generalized as a Naka-Rushton function (see Appendix A). So I decided to create this function to use it in the model.

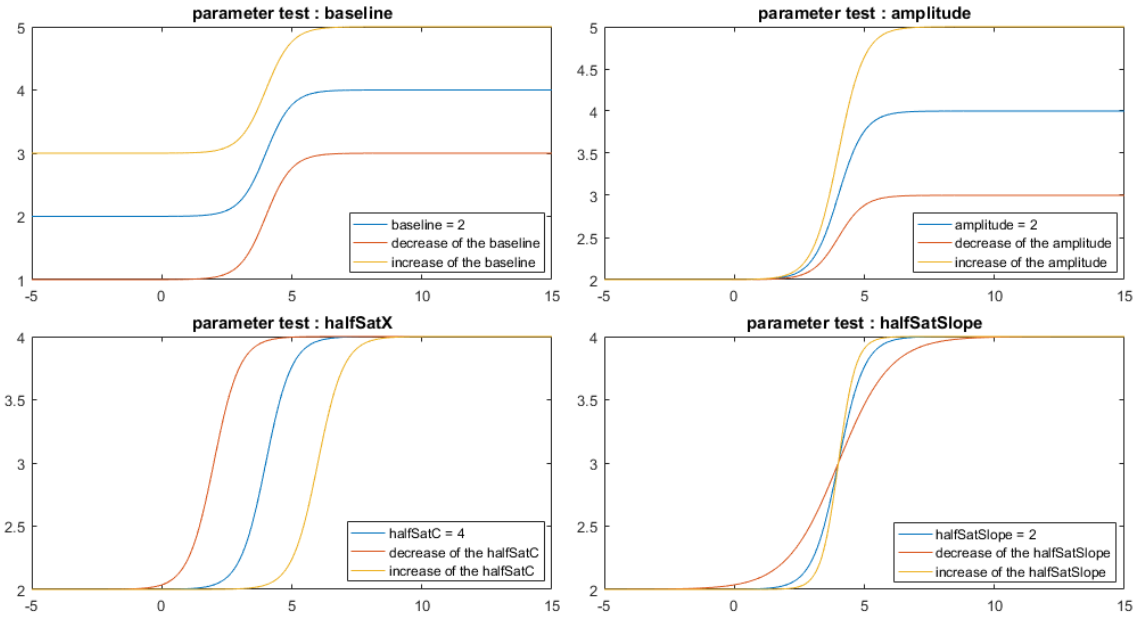

Figure 6.9 – Results of the implemented Naka-Rushton function depending on the varying parameter: (a) b, (b) R_{max}, (c) C_{50} and (d) n.

Implementing this function allowed me not only to lighten the main code by creating a separate function, but also to show the influence of each parameter on the form of the function (see Figure 6.9). This allows us to choose our function input parameters more precisely according to the shape we want to obtain.

The comparison represented in Figure 6.10 shows that the difference between the result of the function and the one from the original program is negligible. Indeed, the absolute difference between the two functions is in the order of 10^{-15}. It is at the limits of numerical calculation accuracy.

This confirms the assumption that the Naka-Rushton function can generalize sigmoid functions.

6.4 The angular distribution function dilemma

In the retina, all the ganglion axons join at the optic disc to form the optic nerve. Experiments have shown that stimulation of a set of retinal cells causes activation of axons in the immediate vicinity. A deformation of the activation profile in the visual cortex is then observed in the opposite direction to the optic disc. Because of the spherical shape of the retina, we assume that the propagation of electrical activity induced by the direct activation of the axons "en passant" can be modeled by an angular distribution centered at the optic disc.

In the original script, a Gaussian angular distribution we used. The goal this

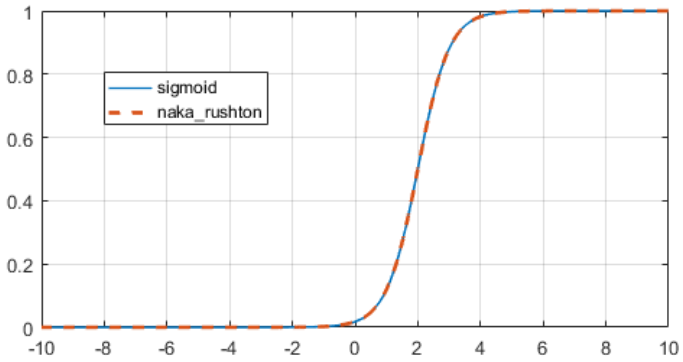

Figure 6.10 – Comparison between the sigmoid (blue line) and the Naka-Rushton (dashed orange line) functions. The difference is negligible because it is at the limits of the computation accuracy (10^{-15}).

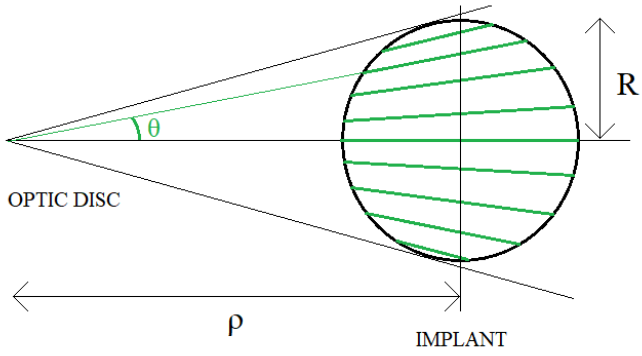

Figure 6.11 – Explanatory diagram of the angular distribution we want to implement in order to model the exponential decay of the quantity of active ganglion axons "en passant". We assume that it is proportional to the distribution as the length of the chords (green lines) as a function of the angle θ

section was to try to define a different distribution and see if it was more accurate.

Let's assume at first that:

- axons form a continuum;
- there is no diffusion around an axon.

The Figure 6.11 represents the simplified form of the angular distribution that we are trying to calculate. The idea is that the number of active axons "en passant" is proportional to the length of the chord of the circle representing the implant. The activation of non-target axons is therefore stronger in the axis formed by connecting the optic disc to the implant, and decreases as it moves away from the implant.

To validate the function that we are going to implement, its results must verify three criteria :

- The maximum amplitude, reached at a zero angle, is equal to the size of the implant;

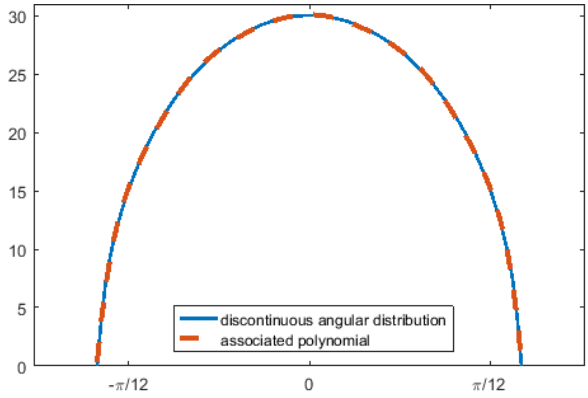

Figure 6.12 – Comparison between the angular distribution plotting and the 10-degree polynomial found with the Matlab function *polyfit*. The absolute difference is negligible.

- The reduction of the maximum angle (cone angle) is a function of distance;
- The distribution is defined on the interval $[-\pi, \pi]$ and is π-periodic.

In order to model the decay of the quantity of active ganglion axons "en passant", the angular distribution has been implemented using two methods:

- By using the Matlab function *linecirc*. This function "finds the points of intersection given a circle defined by a center and radius in x-y coordinates, and a line defined by slope and y-intercept" [5]. After calculating the two end points of the chord, all that remains to calculate is its length;
- By directly calculating the length of the chord, depending on (θ,ρ,R) (see Appendix B). The analytical expression is :

$$L_{\rho,R}(\theta) = 2R \times \sqrt{1 - \frac{\rho^2}{R^2} \times sin^2(\theta)}$$

  where

  - R is the radius of the implant;
  - ρ is the distance of the implant to the optic disc.

  In the implemented function, the angular distribution is calculated over a range of theta in $[-\pi, \pi]$. This function also returns an array of values. So, I had then to use the Matlab function *polyfit* which find the polynomial that is a best fit for the calculated distribution data (Figure 6.12).

The comparison of the results shows a negligible difference between the two methods (at the limit of the accuracy of numerical calculations). However, for more precision, we will use the analytical method.

Afterwards, the implementation of this function produces the results given in Figure 6.13.

However, this angular distribution has limitations. While the hypothesis that axons form a continuum seems consistent with the retinal arrangement, the second hypothesis (no diffusion between axons) was only to simplify the model. It is in fact necessary to take into account a certain diffusion between neighbouring axons. The distribution resulting from taking this into account will no longer have a sharp vanishing at its borders but will show a continuous decrease at the level of the tangents to the implant.

Finally, I compared the Gaussian angular distribution used in the original program to the angular distribution we just calculate (see Figure 6.14).

Unfortunately, I realized that the calculated distribution angle did not match the implant angle. As shown in Figure 6.13, the contours of the cone are not tangent to the circle.

However, due to time constraints, I decided to keep using the Gaussian angular distribution and to return to this calculation later if I had the time.

6.5 Questions about the smoothing parameters

The detailed study of F. Chavane's program led me to question certain points. In particular, retinal and cortical profiles are obtained after application of a smoothing effect.

Firstly, I assumed that the effects due to electrical scattering in the visual cortex and optical scattering of the signal recorded by optical imaging were both represented by the smoothing criterion applied to the profile obtained after retinocortical transformation.

I therefore wondered about the choice of this smoothing criterion.

As mentioned in the section 6.2, one of the main results of this project was the demonstration of a correlation between implant size, the contribution of axons "en passant" and the aspect ratio of simulated cortical activity (see Figure 6.8).

The loop which produces this figure does not allow to directly observe the cortical profiles, so I wrote a code which generates GIF files for each ratio of activated axons "en passant". These figures (For example, Figure 6.15) illustrate the evolution of the profiles according to the size of the implant and for one ratio between 0 and 1.

This shows that for the smallest implant sizes, the profiles are extremely smoothed. Indeed, the surface they occupy is much larger than that of the implant. In addition, as the smoothing matrix is square in shape, the cortical profiles of small implants are

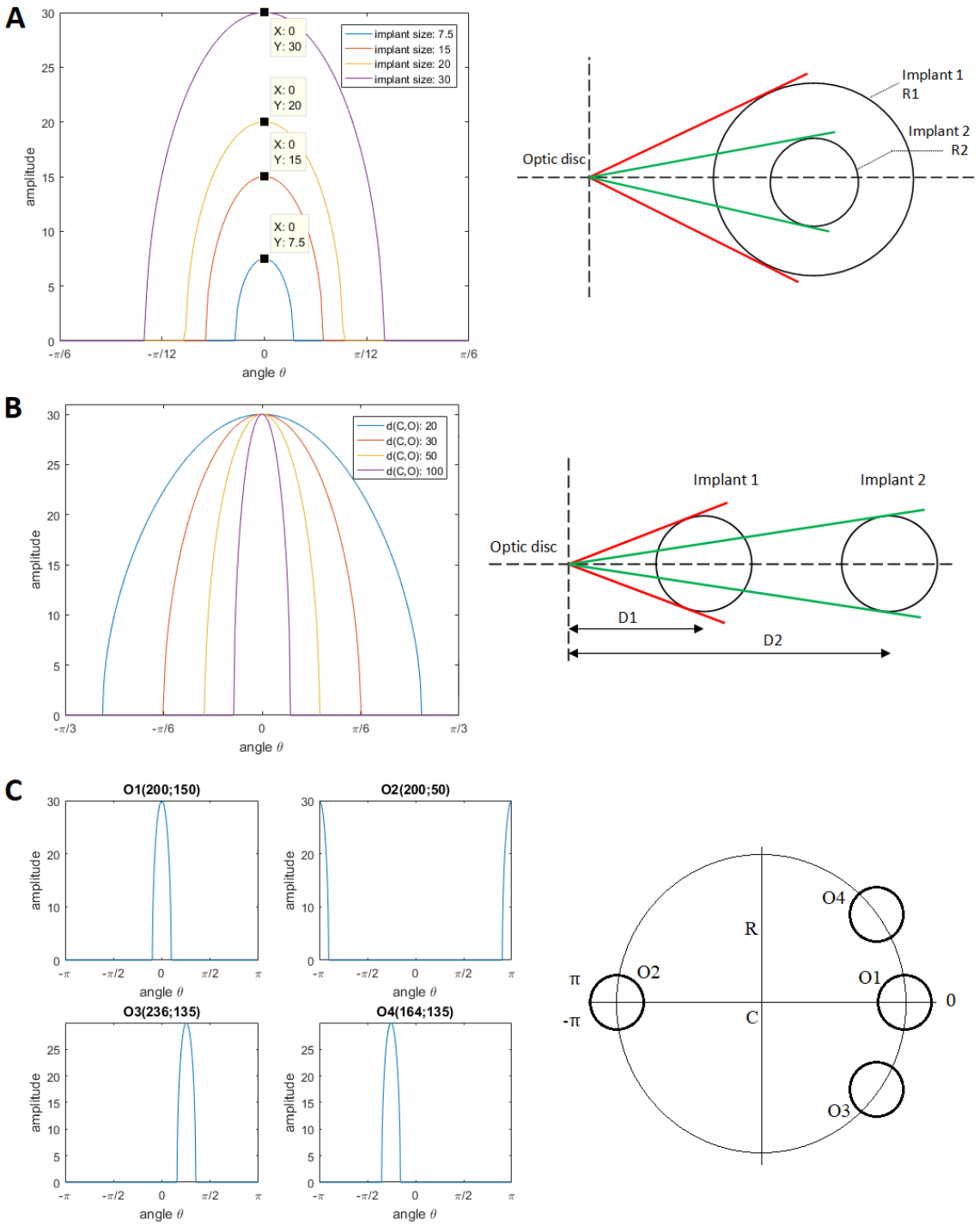

Figure 6.13 – Angular distribution modeling the recruitment of axons "en passant". (A) Effect of the implant size. For the same distance to the optic disc, the angle formed by the implant increase with the radius. Thus, $R_1 > R_2 \Rightarrow \theta_{1,max} > \theta_{2,max}$ (B) Effect of the distance between the optic disc and the implant. For the same radius, the angle formed by the implant decrease with the distance to the optic disc. Thus, $D_1 < D_2 \Rightarrow \theta_{1,max} > \theta_{2,max}$ (C) Effect of the position of the implant relative to the optic disc. In cortical activations obtained by experimentation, the axis from the optic disc to the implant is not necessarily horizontal as in our model. However, we do know the position of the two elements. Thus, the goal here was to generalize angular distribution throughout space. This step also allowed to check the 2π-periodicity of the function. In the case of $O2$, the "separation" of the function is well observed on $[-\pi; \pi]$.

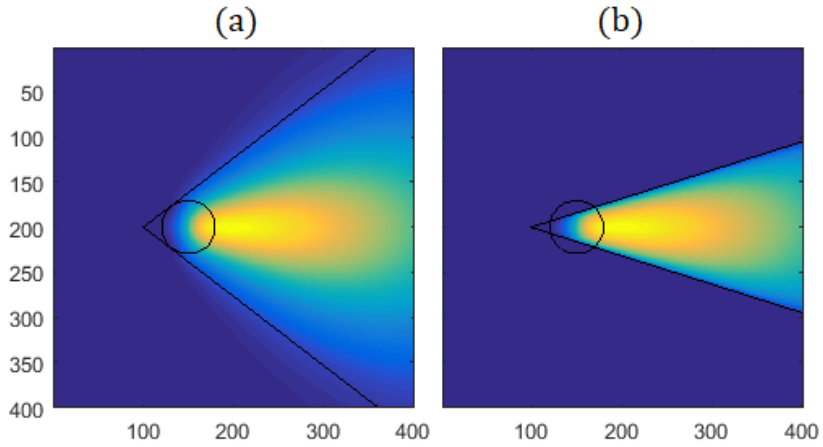

Figure 6.14 – Comparison between (a) the Gaussian angular distribution used in the original program to (b) the angular distribution calculated in this subsection. Note that the range of angular distribution in (b) is not equal to the size of the implant as it should be.

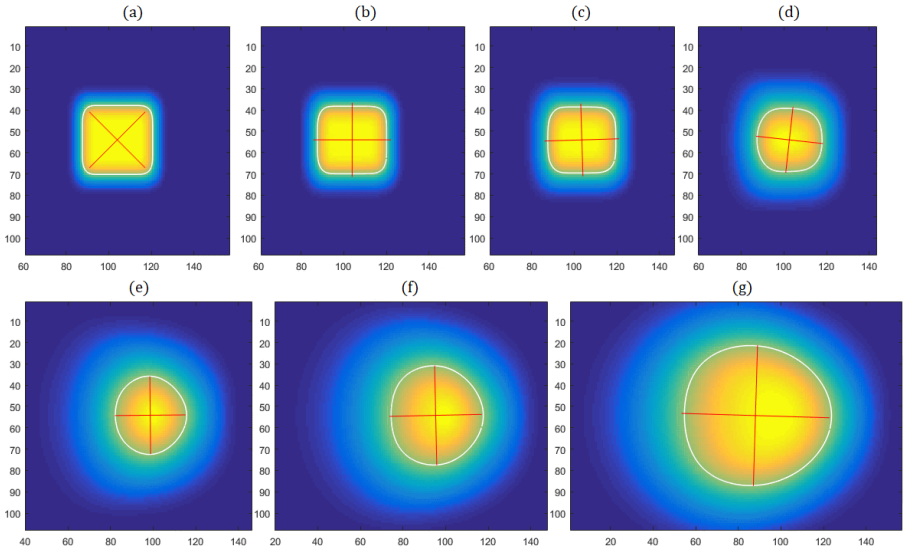

Figure 6.15 – Cortical activations for isotropic "direct" activation only. Ratio of contribution of axons "en passant" is zero. From (a) to (g) the implant varies: 3, 4, 5, 7.5, 15, 20 and 30. There is a clear expansion of cortical activation for small implant sizes due to the high value of the smoothing criterion.

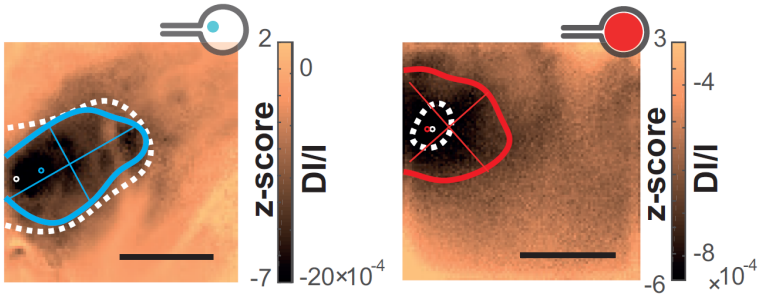

Figure 6.16 – [1] : "Extent of cortical activations generated in 2 animals by SE (blue) and wMEA (red) stimulation at a high current intensity (± 200 and 150 μA respectively) and their corresponding 20° visual stimulus (white dashed contours). Centers of mass of the activation: colored circles; scale bar: 2 mm. The activation amplitude depicted in the colorbar is expressed both in Z-score and in DI/I (unit of measurement used in optical imaging)".

also square in shape and very similar to each other. F. Chavane told me, however, that his choice had been made arbitrarily on the basis of the expected result for the representation of this correlation. The figure being obtained from loop on several criteria, he did not check the shape of the cortical activities for each parameter setting.

Since there was no figure to observe the cortical profiles obtained from the loop execution, I first thought that the arbitrarily chosen value for the smoothing criterion was too high since the profile obtained was much larger than I expected. But when I read again the article [1], I realized that the cortical activity evoked by stimulation of a single electrode (SE) could be as important as a stimulation by the whole implant (wMEA) (see Figure 6.16).

It would still be interesting to see in more detail its influence on the highlighted correlation between implant size, the contribution of axons "en passant" and the aspect ratio of simulated cortical activity.

Secondly, a different criterion is also applied to the retinal profile. However, the two diffusion effects taking place at the level of the retina had already been taken into account. That's why I doubted the interest of this smoothing.

In order to study the importance of this criterion, I compared the retinal profiles obtained with or without its application. The result is shown in Figure 6.17.

We observe a shape that is not spatially uniform, which may be explained by errors of calculation accuracy or model. Moreover, the error value is low before the maximum amplitude of the profiles, which implies that the absolute difference is not significant. In addition, the cortical activations and their mass centers are represented for the contours (black line: with smoothing, white dashed line: without). We notice that they seem superimposed. I therefore concluded that even adding this smoothing criterion do not seem relevant.

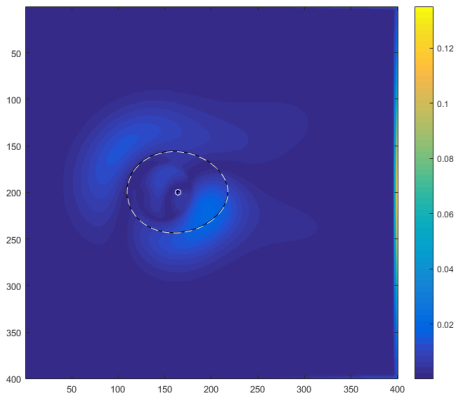

Figure 6.17 – Absolute difference between the retinal activation profile with or without application of a smoothing criterion.

Chapter 7

Objectives of improvements that I have not been able to conduct

7.1 Comparison of the model with experimental data on rat and adaptation of simulation parameters

The experiments made it possible to observe the existence of diffusions in the retina, in the cortex and due to optical imaging. The complete modeling of the system aims to adapt the parameters related to these diffusions in order to get closer to the experimental data.

This parameters adjustment is done by comparing an actual cortical activation with those simulated by a range of values for each parameter. The fit must be made on the following parameters:

- The standard deviation σ_{cone} of the Gaussian angular distribution representing the contribution of the axons "en passant" taking into account the diffusion between axons;
- The ratio α determining the proportion of axons "en passant" active;
- The standard deviation σiso of the isotropic "direct" activation which is modeled by a flat-top Gaussian that corresponds to the diffusion in the aqueous medium separating the retina and the implant, and the diffusion between nearby axons;
- The value ch that determines the activation threshold for defining retinal and cortical profiles;

- The value of the smoothing criterion $N_{smooth,cort}$ at the cortical activation level. This is supposed to take into account the electrical diffusion in the visual cortex as well as the optical diffusion of the signal recorded by optical imaging.

Due the high number of parameters, it is a long and consistent work to put in place that I have not been able to achieve due to lack of time.

7.2 Adaptation to the monkey instead of the rat

The advantage of adapting the rat model to the retinotopy of the monkey is that its retinotopy is close to that of humans. This study may help determine even more precisely the causes of vision deformation when retinal prostheses are used, with the objective of optimizing them.

The calculation of the retinotopy can be done using two methods:

By using cartesian coordinates :

As a reminder, [6] has determined that the map of the visual space in V1, symbolized by the function w, is defined by the following :

$$w(E,P) = k \times log(E \times e^{iPf_a} + a) \tag{7.1}$$

$$\text{where} \begin{cases} E \quad \text{is the retinal eccentricity} \\ P(\theta) = \alpha \times \theta \quad \text{is the angular deviation from the horizontal meridian} \\ f_a(E,P) = sech(P)^{sech(\log E/a \times 0.76) \times 0.1821} \quad \text{is a shear function.} \end{cases}$$

with:

- θ : the original polar angle
- α : a compression parameter reflecting the angular compression along the iso-eccentricity curves
- k : a scaling constant
- a : a structural parameter that defines the limit of the foveal singularity

The Figure 7.1A shows the result obtained from the calculation on cartesian coordinates (k = 10, a =0.52 and α = 0.5). The obtained shape corresponds well to the expected result Figure 7.2C.

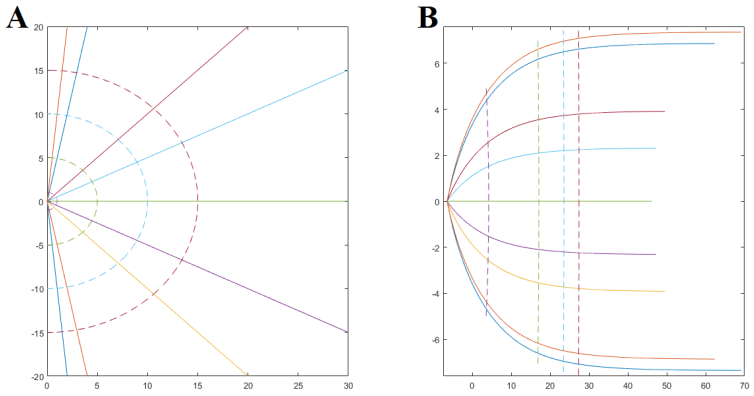

Figure 7.1 – Monkey retino-cortical transformation by calculation from cartesian coordinates. (A) Right part of the retina corresponding to the left part of the visual field. (B) Right hemisphere of the primary visual cortex.

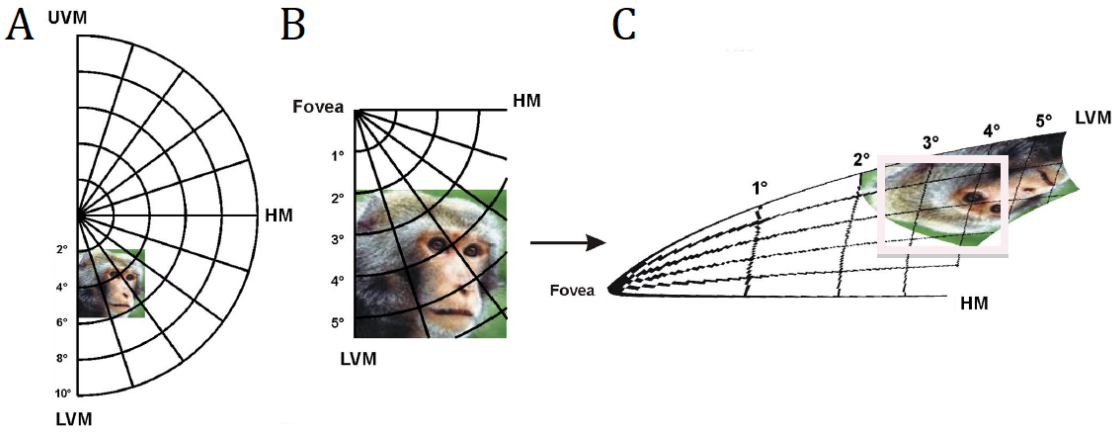

Figure 7.2 – [2] : "Analytical 2D mapping of the visual stimuli onto cortical space. (C) An example of a stimulus as seen in the visual field, shown here against a polar grid. (D) Enlargement of the stimulus zone in (C). (E), The stimulus zone in (D) after applying the analytical spatial transformation. UVM, upper vertical meridian; LVM, lower vertical meridian; HM, horizontal Meridian".

Moreover, the result obtained by applying retinotopy expressed from cartesian coordinates to a simple image seems consistent with the expected shape (see Figure 7.3). Note that the strong cortical magnification of the foveal zone (shown here in blue) is clearly visible.

Unfortunately, the result is imprecise and its computation is very time-consuming.

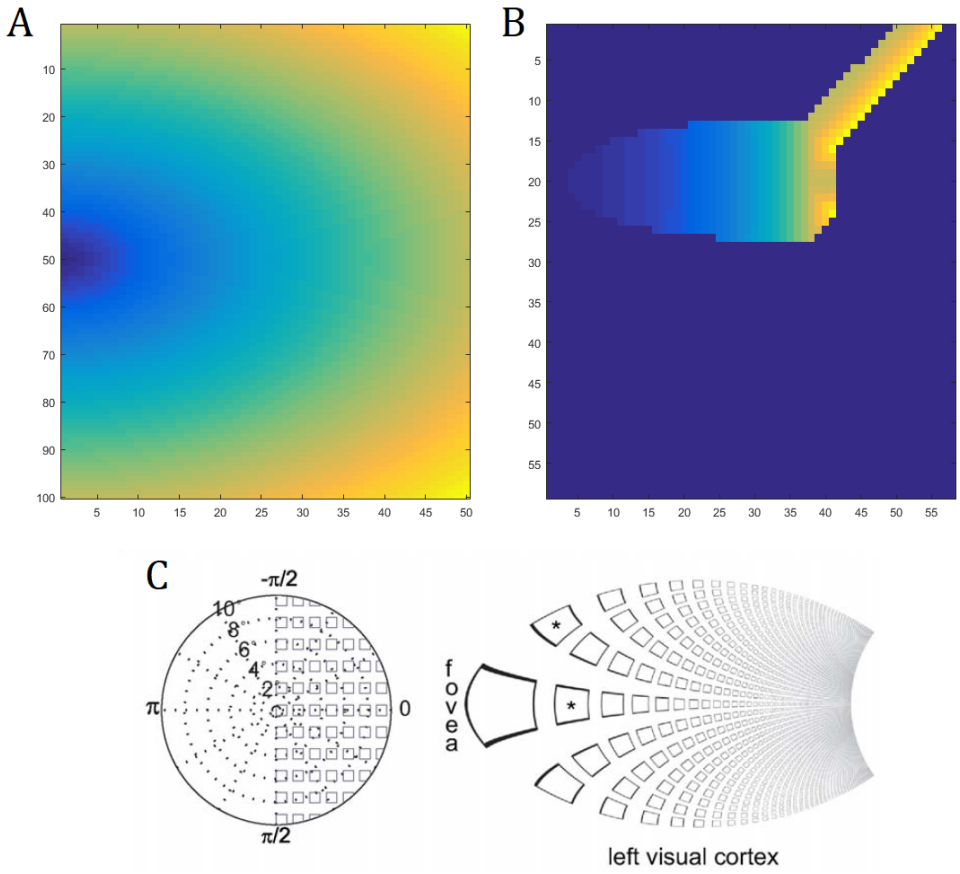

Figure 7.3 – Result of the retinocortical transform on a basic image. The colour code is used to indicate the distance from the fovea.(A) Image on which retino-cortical transformation is applied. (B) Result of the transformation. The resulting image shows that there are numerical problems, or problems in the implementation of the function. However, we can see an elliptical shape close to the expected shape as shown in C. (C) [6] : "Mapping of a set of squares in the right visual field to the left hemisphere V1."

By using polar coordinates :

However, for more accuracy, it is necessary to implement this transform according to polar coordinates. It will then be possible to split the retinal plane into two parts in order to calculate the transforms separately for each hemisphere.

Several issues were raised.

By choosing a constant sampling step on the angle, the greater the distance to the fovea (center of the retina), the less precise the accuracy will be since the points will be more spaced from each other.

In order to obtain a constant spacing, it is therefore necessary to use a variable step depending on the distance from the fovea. For more readability, the calculation of the step, which leads to the expression use for Figure 7.4, will be given in Appendix C .

If using polar coordinates makes the calculation more accurate, the representa-

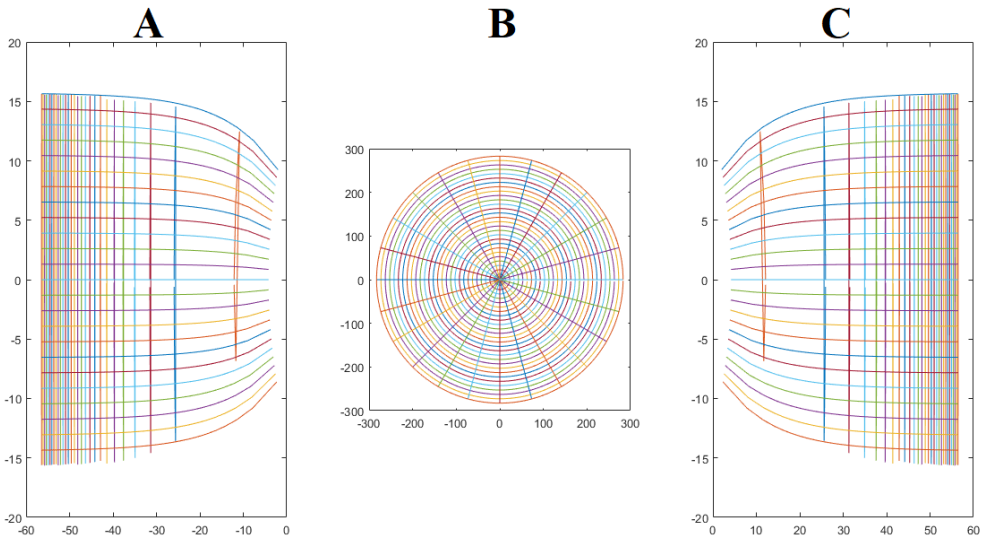

Figure 7.4 – Monkey retino-cortical transformation by calculation from polar coordinates. (A) Left part of the primary visual cortex. (B) Retinal plane. (C) Right part of the primary visual cortex.

tion of the figure is more complex since it requires sorting points according to their position. This is why, for example, all segments leaving the fovea are taken into account, whatever the hemisphere represented (Figure 7.4).

Unfortunately, I did not go any further into this function due to lack of time. I think, however, that the work of [2] would be of great help in achieving this objective. If I think I wasted time trying to implemented the monkey retinotopy, I really became aware of the difficulty of interpreting the result. Getting a result does not mean that it is correct, but only that its refutation has not yet been made, and this is all the more true in the research field.

GENERAL CONCLUSION

The prospects of the study

In terms of perspectives, the finalization of the study remains to be done by adjusting the model parameters in order to fit the cortical activity found to the experimental data.

The adaptation of the model to the monkey would bring it closer to a human model. The effects on the cortical activation obtained could then be studied and, if the experiment carried out on the rat is reproduced on the monkey, this would make it possible to compare the results of the model with experimental data as for the rat model.

The benefits of the internship

This internship was a collaboration between two research centers, thus allowing me to discover two different work places linked by research. My work environment during this period allowed me to be in contact with people with different professional backgrounds (researchers, PhD students, engineers...), which led me to think more about my own career path. Moreover, being in an international environment has not only allowed me to acquire new scientific knowledge, but also to pratice my English.

In terms of computer skills, I was able to apply the knowledge acquired at the ENSEA and acquire new ones. If at beginning I wasn't very confident about my Matlab skills, I quickly realized the effectiveness of the automatisms I acquired during Major Signal's TP-projects. In particular, I realized how important it is to write intelligible and commented codes.

My personal goal as an intern was to learn more about research work. Since I want to specialize in Biomedical Engineering, I wanted to see for myself the difference between an engineer and a researcher in order to know more precisely what fits more my personality.

What I have learned is that research often leads to deciding by oneself what problems to solve. Indeed, one of the major difficulties of research is that the complexity of projects requires a particular methodology which consists in dividing a problem into several sub-problems. If this ability to change approach in the face of the difficulties encountered is acquired with experience, it is all the more complicated to apply in a field such as Research where "a negative result is a result".

I appreciated the autonomy offered by this internship which allowed me to decide on how to manage the resolution of a problem. This sometimes requires creativity, which gives a playful dimension to the project that I particularly enjoyed. However, it also requires being rigorous in defining milestones to follow, which is the main problem I have encountered. This is why it sometimes happens to get literally lost

in reflections, which unfortunately do not always lead to concrete results.

Consequently, it led me to take a new look at my career plan by asking myself what I really wanted to do, and by thinking not only of my professional expectations but also on their impact on my personal life.

Appendix A

Calculation of the generalization of a sigmoid function by a Naka-Rushton function

A sigmoid function is defined by the formula :

$$S(x) = \frac{1}{1+e^{-x}} = \frac{e^x}{1+e^x}$$

We will demonstration that it is possible to generalize this expression by a Naka-Rushton function (*Naka and Rushton, 1966*), which is defined as follows.

$$Response = R_{max} \times \frac{C^n}{C^n + C_{50}^n} + b$$

with:

- b : the baseline (background discharge)
- R_{max} : the maximum response for a baseline of null value
- C_{50} : the level of contrast which produces half of R_{max} (constant of semi-saturation)
- n: dimensionless constant that controls the slope of the curve at a contrast of C_{50}

Demonstration

We set : x = ln(C), then :

$$C = e^x$$

And :

$$Response = R_{max} \times \frac{e^{xn}}{e^{xn} + e^{x_{50}n}} + b$$

$$= R_{max} \times \frac{\frac{e^{xn}}{e^{x_{50}n}}}{\frac{e^{xn}}{e^{x_{50}n}} + 1} + b$$

$$= R_{max} \times \frac{e^{(x-x_{50})n}}{1 + e^{(x-x_{50})n}} + b$$

$$= R_{max} \times \frac{1 + e^{(x-x_{50})n} - 1}{1 + e^{(x-x_{50})n}} + b$$

Finally,

$$Response = (R_{max} + b) - R_{max} \times (1/(1 + e^{(n \times (x-x_{50}))})$$

This final expression was tested and confirmed by comparing the sigmoid used in the code with the result of the **naka_rushton.m** function created (see Figure 6.10).

Appendix B

Calculation of the angular distribution

Because of the spherical shape of the retina, the propagation of electrical activity induced by the direct activation of the axons "en passant" can be modeled by an angular distribution.

The angular distribution that we want to implement assume that the number of active axons "en passant" is proportional to the length of the chord of the circle representing the implant. The activation of non-target axons is therefore stronger in the axis formed by connecting the optic disc to the implant, and decreases as it moves away from the implant. Figure B.1 gives the schema used in the calculation.

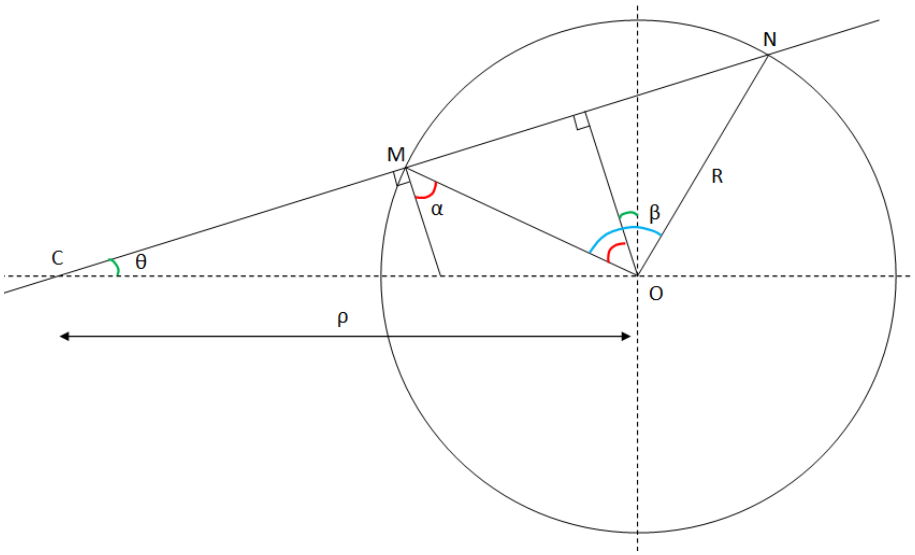

Figure B.1 – Schema defining the different variables used in the calculation.

Goal : calculate the length of $L = MN$, chord set as depending on (θ, ρ, R)

$$\text{Where} : \begin{cases} \theta & \text{is the angle between the chord and the horizontal;} \\ R & \text{is the radius of the implant;} \\ \rho & \text{is the distance of the implant to the optic disc.} \end{cases}$$

In COM triangle :

$$\text{Law of sines :} \quad \frac{sin\left(\frac{\pi}{2}+\alpha\right)}{CO} = \frac{sin(\theta)}{OM}$$

$$\text{Hence,} \quad \frac{cos(\alpha)}{\rho} = \frac{sin(\theta)}{R}$$

In MON triangle :

$$\text{Law of sines :} \quad \frac{sin\left(\frac{\pi}{2}-\alpha\right)}{ON} = \frac{sin(\beta)}{MN}$$

$$\text{But} : \begin{cases} \beta = 2\alpha \quad \text{(Isosceles triangle + bisector)} \\ sin(2\alpha) = 2sin(\alpha)cos(\alpha) \end{cases}$$

$$\text{Hence,} \quad \frac{cos(\alpha)}{R} = \frac{2sin(\alpha)cos(\alpha)}{L}$$

Calculation of the chord length :

$$L = 2Rsin(\alpha)$$

$$sin(\alpha) = \sqrt{1 - \left(\frac{\rho}{R}sin(\theta)\right)^2}$$

Hence finally :

$$L_{\rho,R}(\theta) = 2R \times \sqrt{1 - \frac{\rho^2}{R^2} \times sin^2(\theta)}$$

Appendix C

Calculation of the sampling step used in the implementation of the monkey retinocortical transform

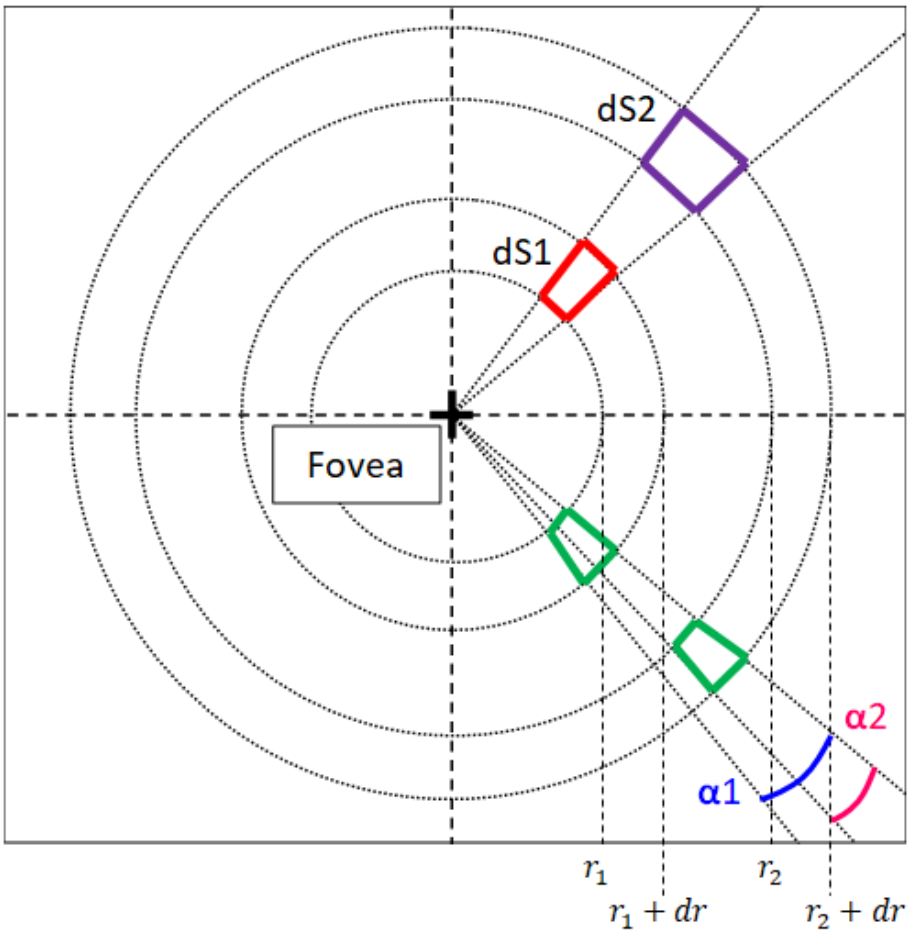

Figure C.1 – Schema defining the different variables used in the calculation.

In order to implement the monkey retinotopy, a loop is made on the distance from the fovea and the angle from the vertical axis. Indeed, the retinal plane is not treated as a whole : its right part is treated by the left hemisphere of the visual cortex and vice versa. This is why the range of definition of the angle will be $[-\frac{\pi}{2}; \frac{3\pi}{2}]$.

Two methods can be used.

By using a constant step :

As shown in the upper right part of the diagram Figure C.1, the elementary surfaces $dS1$ and $dS2$ are not equivalent according to the distance to the fovea.

This is why for two different distance r_1 and r_2, two consecutive points will not have the same spacing.

Thus, the calculation accuracy of the transform decreases with the distance to the fovea.

By using a variable step depending on the distance to the fovea :

This can be corrected by using a variable step (in the lower right part of the diagram).

Goal : For a fixed (r_1, r_2, dr), one wants to obtain the following equality : $dS1 = dS2$

Knowing that:

$$dS = rD\theta dr$$

The result one wants to obtain is:

$$r_1 d\theta_1 = r_2 d\theta_2$$

To calculate the step of the angle for a given r, it is enough to choose it equal to dr/r' with r' the consecutive value to r in the loop.

Bibliography

[1] S. Roux et al., *Probing the functional impact of sub-retinal prosthesis*. eLife 2016; DOI:10.7554/eLife.12687

[2] Inbal Ayzenshtat, Ariel Gilad, Guy Zurawel, and Hamutal Slovin. *Population Response to Natural Images in the Primary Visual Cortex Encodes Local Stimulus Attributes and Perceptual Processing*. The Journal of Neuroscience, October 2012.

[3] C. Gias et al., *Retinotopy within rat primary visual cortex using optical imaging*. NeuroImage 24 (2005) 200– 206.

[4] Bruno Cessac, *Retinal disorders and therapy* Report for the creation of the BIOVISION team, April 2018

[5] MathWorks website (MathWorks is the editor of the Matlab mathematical computing software), *https://fr.mathworks.com/*

[6] Schira at al., *Modeling Magnification and Anisotropy in the Primate Foveal Confluence*. PLoS Computational Biology, January 2010

[7] Adrien Wohrer, *Model and large-scale simulator of a biological retina, with contrast gain control*. PhD Thesis, 2008

[8] Bruno Cessac, *The retina a fascinating object of study for a physicist*. UCA COMPLEX DAYS, In press, 2018. <hal-01807518>

[9] Molday RS et al., *Photoreceptors at a glance*. J Cell Sci 128, 2015

[10] National Eye Institute website, *https://nei.nih.gov/health/maculardegen/armd_facts*

[11] Trevor Huffa and Scott C. Dulebohn, *Neuroanatomy, Visual Cortex* NCBI (National Center for Biotechnology Information), 2018